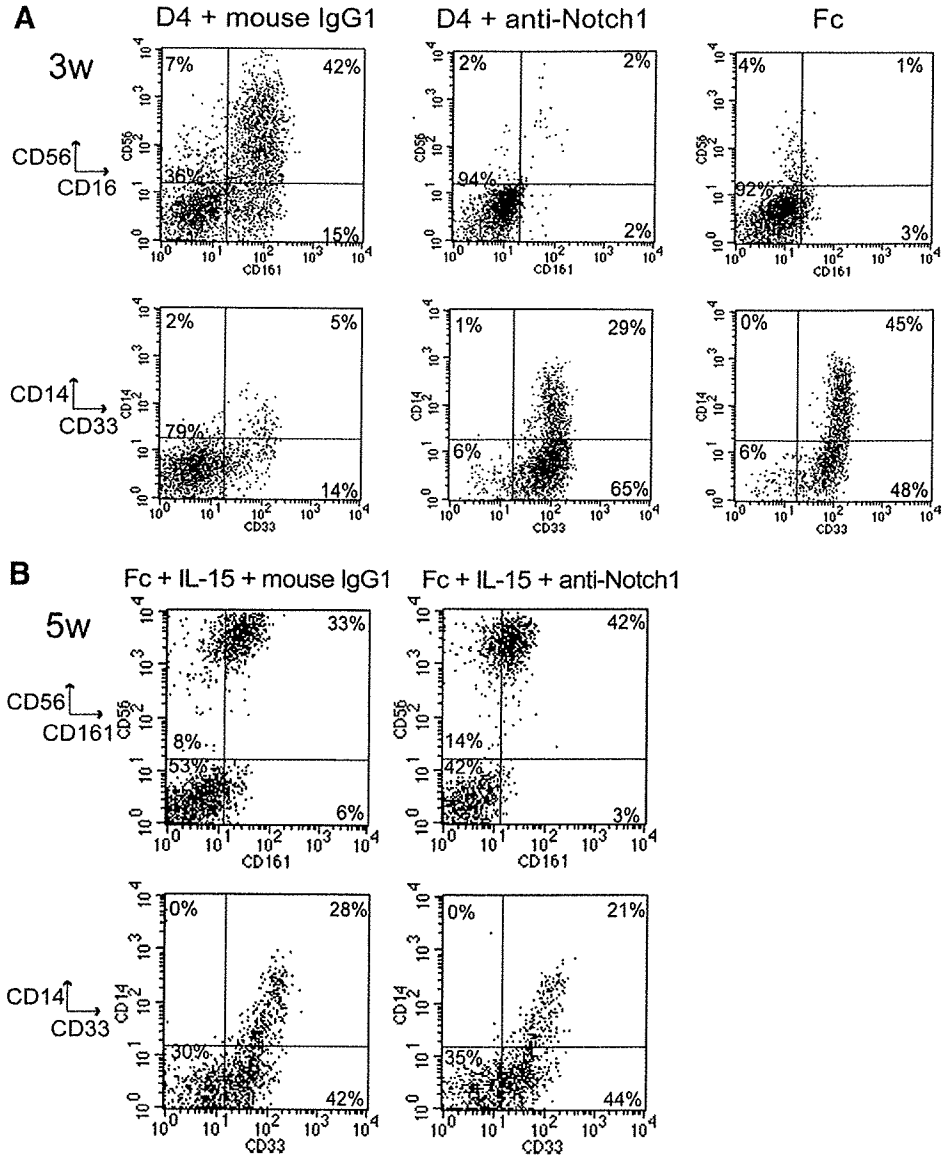

FIGURE 6. Phenotypic analysis of cells cultured in the presence of human Notch1-blocking Ab. *A*, Representative dot plots of cells that were cultured for 3 wk from CB CD34$^+$ cells on Delta4-Fc-coated plates with mouse IgG1-containing medium, Delta4-Fc-coated plates with anti-human Notch1-containing medium, and Fc-coated plates. Results are representative of six experiments. *B*, Representative dot plots of cells that were cultured for 5 wk from CB CD34$^+$ cells on Fc-coated plates with IL-15 and mouse IgG1-containing medium and Fc-coated plates with IL-15 and anti-human Notch1-containing medium. Results are representative of three experiments.

progenies to the CD161$^+$CD7$^+$ NK cell fate within 2 wk, presumably before CD161$^+$ is expressed.

IL-15, along with Delta4 stimulation, induces phenotypic maturation and functional augmentation of CB CD34$^+$ cell-derived NK cells

We compared the immunophenotype of the CB CD34$^+$ cell-derived NK cells generated in the culture with Delta4-Fc but lacking IL-15 (D4-Fc) and in culture with Delta4-Fc and IL-15 (D4-Fc plus IL-15). IL-15 does not affect the absolute cell number; fold increases in the cell number after the 3-wk culture were 10.6 ± 6.16-fold and 10.2 ± 6.71-fold with and without IL-15 in the D4-Fc-coated plate condition (n = 8). The cells grew slightly faster with D4-Fc plus IL-15 than with D4-Fc alone, but there were no significant differences in the frequency of CD56$^+$CD161$^+$ population in both conditions after 3 wk (cf Fig. 3 and supplemental Fig. S2*A*, D4-Fc and D4-Fc plus IL-15; supplemental Fig. S2*Bii*; and Fig. 5). The expression levels of CD7 and NKG2D were similar. CD94 was expressed at a higher level in the D4-Fc plus IL-15 condition. CD16 and CD158 were not expressed in the D4-Fc condition, but were expressed at low levels in the D4-Fc plus IL-15 condition. The expression levels of adhesion molecules, i.e., CD11a, CD11b, and CD62L, were higher in the D4-Fc condition (Fig. 5*A*). The other markers shown in Fig. 1 (CD2, CD7, CD25, CD27, CD44, CD45RA, CD57, CD117, CD122, and CCR7; data not shown), as well as IFN-γ (Fig. 5*D*), were expressed at similar levels under both conditions. There was a remarkable difference in the expression level of CD56, which was markedly higher in the D4-Fc plus IL-15 condition.

Cytotoxic activity against K562 cells was significantly higher in NK cells generated in the D4-Fc plus IL-15 condition than that in the D4-Fc condition. CMA, an inhibitor of perforin-mediated cytotoxicity, had a stronger suppressive effect on the cytotoxic activities of NK cells generated in the D4-Fc plus IL-15 condition (Fig. 5*Bi*). Interestingly, granzyme B, which enhances the perforin-mediated cytotoxicity and whose expression was not detected in the D4-Fc condition, was up-regulated in the D4-Fc plus IL-15 condition (Fig. 5*Ci*). This might explain the stronger suppression of NK cell cytotoxic activity by CMA when generated in the D4-Fc plus IL-15 condition compared with the D4-Fc condition. In contrast, there was no significant difference in the killing activities against Jurkat cells of the NK cells generated under

Downloaded from www.jimmunol.org on May 24, 2010

either condition (Fig. 5*Bii*), and CMA did not affect the cytotoxic activities against Jurkat cells, irrespective of the culture conditions (data not shown). This finding suggests that perforin or granzyme B does not have a major role in killing Jurkat cells. We evaluated whether TRAIL had a role by adding anti-TRAIL-blocking Ab RIK2 to the medium. RIK2 partially but clearly suppressed the cytotoxic activities against Jurkat cells generated in both conditions without significant differences (Fig. 5*Bii*), although TRAIL expression was slightly higher in the NK cells generated in the D4-Fc plus IL-15 condition (Fig. 5*Cii*). From these observations, we concluded that IL-15 does not influence the killing activity through TRAIL but does enhance the killing activity through perforin/granzyme B. The cytotoxic activity of immature NK cells is TRAIL dependent, while that of mature NK cells is mainly dependent on perforin (29). Therefore, IL-15 might contribute to the maturation of NK cells and confer on them the capacity to exact perforin/granzyme B-medicated cytotoxicity.

Inhibitory effect of anti-Notch1 Ab on Delta4-dependent NK cell development

We prepared mAbs specific for the extracellular domain of Notch1, Notch2, and Notch3 (supplemental Fig. S4*A*). The expression patterns of Notch1, Notch2, and Notch3 in fresh CB mononuclear cells, $CD34^+$ cells, and products during the culture of $CD34^+$ cells are shown in supplemental Fig. S3, *A* and *B*. Notch1 was expressed at higher levels on NK and T cells than on B cells and monocytes. Notch2 was expressed at higher levels on monocytes than on lymphocytes. Notch3 expression was virtually negative on all types of lymphocytes and positive on monocytes. Notch1 and Notch2, but not Notch3, were expressed on $CD34^+$ cells. The $CD34^+$ cell-derived $CD56^+$ NK cells also expressed Notch1 and Notch2, but not Notch3. All three Notch receptors were expressed on cells grown on the control Fc-coated plates (supplemental Fig. S3*B*).

Because $CD34^+$ cells expressed Notch1 and Notch2, but not Notch3 (supplemental Fig. S3*B*), and the established anti-Notch1 Ab, but not anti-Notch2 Ab, blocked binding of the cognate soluble Notch receptor to the ligands (supplemental Fig. S4*B*), we cultured CB $CD34^+$ cells on Delta4-Fc-coated plates in anti-Notch1 Ab-containing medium. Remarkably, the immunophenotype of the cells grown under the presence of anti-Notch1 Ab was almost the same as that of cells grown on control Fc-coated plates, indicating that the effect of Delta4 was completely blocked and NK cell development was shut down by the anti-Notch1 Ab (Fig. 6*A*). Anti-Notch2 Ab did not have such an effect, consistent with the fact that it did not block ligand binding to the cognate receptors (data not shown). CB $CD34^+$ cells cultured with IL-15 on Fc-coated plates in the presence of the anti-Notch1 Ab gave rise to NK cells in a manner indistinguishable from that of cells grown without the Ab (Fig. 6*B*). These results suggest that Notch1 might be a physiologic Notch receptor that mediates Delta4 signaling for NK cell development from CB $CD34^+$ cells and further support the notion that Notch signaling has a role distinct from that of IL-15.

Discussion

In the present study, we demonstrated that functional NK cells developed from CB $CD34^+$ cells when stimulated with the Notch ligand Delta4. Previous reports indicated that NK cells can be derived from in vitro culture of human $CD34^+$ cells prepared from fetal liver, bone marrow, or CB with either IL-2 or IL-15 (30–33), which signal through the shared IL-2/IL-15 receptor β-chain and the common γ-chain. IL-15 has been considered to have a more physiologic role than IL-2 in NK development (30). Notably, IL-15-independent NK cell differentiation has recently been published (6). This culture system, however, has been reported to be stromal cell dependent while the potential molecules and signaling pathways are unknown and, thus, the conclusion whether IL-15 is indispensable is yet to be determined. Notch signaling has been examined in the context of NK cell development as well and appears to affect the very early phase of progenitor development (17–19). In studies of human NK cell development, however, culture systems containing IL-15 and/or a coculture system with the fetal thymus organ or stromal cells are used exclusively. A novel and unexpected finding in the present study was the fact that stimulation of CB $CD34^+$ cells with a soluble Notch ligand, Delta4-Fc, coated onto the plate in the presence of stem cell factor, FL, and IL-7 was sufficient to induce the development of functional NK cells.

Our data do not officially exclude the possibility that endogenous IL-15 is involved in NK cell development in a manner, e.g., that cell-autonomously produced IL-15 activated the signaling by binding to the receptor intracellularly. Given the fact, however, that the exogenous addition of IL-15 resulted in the qualitative rather than quantitative difference in the NK cells developed in the presence of Delta4-Fc, in addition to inefficient blockade by anti-IL-15-neutralizing Ab, IL-15 is likely to be dispensable for human NK cell development in the presence of Delta4-Fc.

The finding that IL-15 is not necessary for human NK cell development in culture contrasts with the absolute necessity of IL-15 signaling for NK development in some mouse phenotypes; mice lacking a gene for IL-15 (3) (34, 35), IL-15 receptor α-chain (36), common β-chain (37), or common γ-chain (38, 39) lack NK cells. This might be due to differences between the in vitro culture conditions and the in vivo environment in which NK cells develop. Another explanation might be a difference between mice and humans, as in the case of IL-7 requirement for T cell development; IL-7 is required for the V-D-J rearrangement of the TCR β-chain gene in humans, whereas it is dispensable in mouse T cell development (40).

Previous studies reported that the effect of Notch signaling in the presence of IL-15 on NK cell development is confined to the very early stages of development. In the present study, we demonstrated that Notch signaling confers CD7 expression competence on cells cultured with or without IL-15 for 1 wk or less, but not for 2 wk, unless also stimulated by Notch. This finding is similar to that in a previous report demonstrating that Notch signaling confers cyCD3 expression competence only on prethymic but not thymic NK cell progenitors or peripheral blood $cyCD3^-$ NK cells (19). We confirmed the Notch signal dependency of cyCD3 expression during NK cell development. Coexpression of CD7 and CD45RA on $CD34^+$ cells might be associated with a restriction toward NK cell development (26, 33). Our data strongly suggest that the vast majority, if not all, of the NK cells derived from $CD34^+$ cells without Notch signaling were generated through $CD7^-$ cells. Therefore, although it is yet to be elucidated whether all of the NK cell progenitors are $CD7^+$ (41), NK cells established in vitro without Notch stimulation might not develop from a physiologic NK progenitor or might skip the physiologic NK/T progenitor stage. Furthermore, our data suggest that the effect of Notch stimulation on CD7 expression is imprinted on cells only if it is administered at the initial stage of the $CD34^+$ cell culture. We, however, failed to prospectively identify the subpopulations in the $CD34^+$ cells that are targets of Delta4 to develop NK-lineage cells. Delta4 stimulation induced NK cell development from both the most immature $CD34^+CD38^-$ and more mature $CD34^+CD38^+$ progenitor populations and both $CD34^+$

Downloaded from www.jimmunol.org on May 24, 2010

$CD45RA^+$ lymphoid progenitors and $CD34^+CD45RA^-$ populations (data not shown).

The findings of the present study extend our understanding to more mature stages of NK cell differentiation: the presence of Notch signaling induces generation of functional NK cells in culture conditions that do not generate $CD56^+$ cells without Notch stimulation per se. The precise stages of NK cell development during which Notch signaling determines the progression toward functional NK cells is not known.

In our experiments, even cells cultured with a Notch ligand alone had cytotoxic activity. The level of this activity, however, was weaker than that in NK cells generated by Notch stimulation with IL-15. Indeed, the perforin-mediated cytotoxicity of NK cells generated in the absence of IL-15 was significantly weaker, despite the fact that this is the major pathway of mature NK cells to kill target cells (42). In contrast, the TRAIL-mediated cytotoxicity was almost the same regardless of presence or absence of IL-15. This finding, along with the change in the expression level of CD56, might indicate that IL-15 induces the maturation of $CD56^{low}$ $CD161^+$ immature NK cells generated by Notch stimulation without IL-15. Another difference between the cells cultured with or without IL-15 was the down-regulation of adhesion molecules (CD11a, CD11b, CD62L) on the cell surface. These molecules might be important for homing of the NK cells to the sites at which they function.

To our surprise, cytotoxic activities were not detected in the cell populations generated in the control Fc plus IL-15 condition at either 3 or 6 wk (Fig. 5*B* and data not shown), although these results might be affected by the facts that the frequency of $CD56^+CD161^+$ cells was very low at 3 wk and that culture for 6 wk might be too long to evaluate cytotoxic activities while the frequency of $CD56^+CD161^+$ cells was much greater. In any case, when clinical application of progenitor-derived NK cells is considered, a Delta4-Fc-coating system would give a significant advantage.

In conclusion, Notch stimulation by Delta4 (or Delta1) was required for initial NK cell differentiation and the development of $CD161^+CD56^{low}$ immature NK cells. Among Notch receptors, Notch1 might be essential for physiologic NK cell development, although the involvement of other Notch receptors is yet to be elucidated. IL-15 was not essential for differentiation, but was necessary for maturation. IL-15 might have an indispensable role only in the later part of the NK development. This knowledge might be useful for future approaches toward the ex vivo generation and manipulation of NK cells and their therapeutic application.

Acknowledgments

We thank Y. Mori and E. Nakasone for providing excellent technical assistance.

Disclosures

The authors have no financial conflict of interest.

References

1. Freud, A. G., and M. A. Caligiuri. 2006. Human natural killer cell development. *Immunol. Rev.* 214: 56–72.
2. Hayakawa, Y., N. D. Huntington, S. L. Nutt, and M. J. Smyth. 2006. Functional subsets of mouse natural killer cells. *Immunol. Rev.* 214: 47–55.
3. Kennedy, M. K., M. Glaccum, S. N. Brown, E. A. Butz, J. L. Viney, M. Embers, N. Matsuki, K. Charrier, L. Sedger, C. R. Willis, et al. 2000. Reversible defects in natural killer and memory CD8 T cell lineages in interleukin 15-deficient mice. *J. Exp. Med.* 191: 771–780.
4. Williams, N. S., J. Klem, I. J. Puzanov, P. V. Sivakumar, J. D. Schatzle, M. Bennett, and V. Kumar. 1998. Natural killer cell differentiation: insights from knockout and transgenic mouse models and in vitro systems. *Immunol. Rev.* 165: 47–61.
5. Yokoyama, W. M., S. Kim, and A. R. French. 2004. The dynamic life of natural killer cells. *Annu. Rev. Immunol.* 22: 405–429.
6. McCullar, V., R. Oostendorp, A. Panoskaltsis-Mortari, G. Yun, C. T. Lutz, J. E. Wagner, and J. S. Miller. 2008. Mouse fetal and embryonic liver cells differentiate human umbilical cord blood progenitors into CD56-negative natural killer cell precursors in the absence of interleukin-15. *Exp. Hematol.* 36: 598–608.
7. Chiba, S. 2006. Concise review: Notch signaling in stem cell systems. *Stem Cells* 24: 2437–2447.
8. Artavanis-Tsakonas, S., M. D. Rand, and R. J. Lake. 1999. Notch signaling: cell fate control and signal integration in development. *Science* 284: 770–776.
9. Suzuki, T., and S. Chiba. 2005. Notch signaling in hematopoietic stem cells. *Int. J. Hematol.* 82: 285–294.
10. Radtke, F., A. Wilson, G. Stark, M. Bauer, J. v. Meerwijk, H. R. MacDonald, and M. Aguet. 1999. Deficient T cell fate specification in mice with an induced inactivation of Notch1. *Immunity* 10: 547–558.
11. Wilson, A., H. R. MacDonald, and F. Radtke. 2001. Notch 1-deficient common lymphoid precursors adopt a B cell fate in the thymus. *J. Exp. Med.* 194: 1003–1012.
12. Pui, J. C., D. Allman, L. Xu, S. DeRocco, F. G. Karnell, S. Bakkour, J. Y. Lee, T. Kadesch, R. R. Hardy, J. C. Aster, and W. S. Pear. 1999. Notch1 expression in early lymphopoiesis influences B versus T lineage determination. *Immunity* 11: 299–308.
13. Jaleco, A. C., H. Neves, E. Hooijberg, P. Gameiro, N. Clode, M. Haury, D. Henrique, and L. Parreira. 2001. Differential effects of Notch ligands Delta-1 and Jagged-1 in human lymphoid differentiation. *J. Exp. Med.* 194: 991–1002.
14. De Smedt, M., I. Hoebeke, K. Reynvoet, G. Leclercq, and J. Plum. 2005. Different thresholds of Notch signaling bias human precursor cells toward B-, NK-, monocytic/dendritic-, or T-cell lineage in thymus microenvironment. *Blood* 106: 3498–3506.
15. van den Brandt, J., K. Voss, M. Schott, T. Hunig, M. S. Wolfe, and H. M. Reichardt. 2004. Inhibition of Notch signaling biases rat thymocyte development towards the NK cell lineage. *Eur. J. Immunol.* 34: 1405–1413.
16. Garcia-Peydro, M., V. G. de Yebenes, and M. L. Toribio. 2006. Notch1 and IL-7 receptor interplay maintains proliferation of human thymic progenitors while suppressing non-T cell fates. *J. Immunol.* 177: 3711–3720.
17. Rolink, A. G., G. Balciunaite, C. Demoliere, and R. Ceredig. 2006. The potential involvement of Notch signaling in NK cell development. *Immunol. Lett.* 107: 50–57.
18. Carotta, S., J. Brady, L. Wu, and S. L. Nutt. 2006. Transient Notch signaling induces NK cell potential in Pax5-deficient pro-B cells. *Eur. J. Immunol.* 36: 3294–3304.
19. De Smedt, M., T. Taghon, I. Van de Walle, G. De Smet, G. Leclercq, and J. Plum. 2007. Notch signaling induces cytoplasmic CD3ε expression in human differentiating NK cells. *Blood* 110: 2696–2703.
20. Karanu, F. N., B. Murdoch, T. Miyabayashi, M. Ohno, M. Koremoto, L. Gallacher, D. Wu, A. Itoh, S. Sakano, and M. Bhatia. 2001. Human homologues of Delta-1 and Delta-4 function as mitogenic regulators of primitive human hematopoietic cells. *Blood* 97: 1960–1967.
21. Kayagaki, N., N. Yamaguchi, M. Nakayama, A. Kawasaki, H. Akiba, K. Okumura, and H. Yagita. 1999. Involvement of TNF-related apoptosis-inducing ligand in human $CD4^+$ T cell-mediated cytotoxicity. *J. Immunol.* 162: 2639–2647.
22. Kataoka, T., N. Shinohara, H. Takayama, K. Takaku, S. Kondo, S. Yonehara, and K. Nagai. 1996. Concanamycin A, a powerful tool for characterization and estimation of contribution of perforin- and Fas-based lytic pathways in cell-mediated cytotoxicity. *J. Immunol.* 156: 3678–3686.
23. Shimizu, K., S. Chiba, K. Kumano, N. Hosoya, T. Takahashi, Y. Kanda, Y. Hamada, Y. Yazaki, and H. Hirai. 1999. Mouse Jagged1 physically interacts with Notch2 and other Notch receptors. *J. Biol. Chem.* 274: 32961–32969.
24. Geling, A., H. Steiner, M. Willem, L. Bally-Cuif, and C. Haass. 2002. A γ-secretase inhibitor blocks Notch signaling in vivo and causes a severe neurogenic phenotype in zebra fish. *EMBO Rep.* 3: 688–694.
25. Cheng, H.-T., J. H. Miner, M. Lin, M. G. Tansey, K. Roth, and R. Kopan. 2003. γ-Secretase activity is dispensable for mesenchyme-to-epithelium transition but required for podocyte and proximal tubule formation in developing mouse kidney. *Development* 130: 5031–5042.
26. Haddad, R., P. Guardiola, B. Izac, C. Thibault, J. Radich, A.-L. Delezoide, C. Baillou, F. M. Lemoine, J. C. Gluckman, F. Pflumio, and B. Canque. 2004. Molecular characterization of early human T/NK and B-lymphoid progenitor cells in umbilical cord blood. *Blood* 104: 3918–3926.
27. Sanchez, M., M. Muench, M. Roncarolo, L. Lanier, and J. Phillips. 1994. Identification of a common T/natural killer cell progenitor in human fetal thymus. *J. Exp. Med.* 180: 569–576.
28. Huntington, N. D., C. A. J. Vosshenrich, and J. P. Di Santo. 2007. Developmental pathways that generate natural-killer-cell diversity in mice and humans. *Nat. Rev. Immunol.* 7: 703–714.
29. Zamai, L., M. Ahmad, I. M. Bennett, L. Azzoni, E. S. Alnemri, and B. Perussia. 1998. Natural killer (NK) cell-mediated cytotoxicity: differential use of TRAIL and Fas ligand by immature and mature primary human NK cells. *J. Exp. Med.* 188: 2375–2380.
30. Mrozek, E., P. Anderson, and M. Caligiuri. 1996. Role of interleukin-15 in the development of human $CD56^+$ natural killer cells from $CD34^+$ hematopoietic progenitor cells. *Blood* 87: 2632–2640.
31. Jaleco, A., B. Blom, P. Res, K. Weijer, L. Lanier, J. Phillips, and H. Spits. 1997. Fetal liver contains committed NK progenitors, but is not a site for development of $CD34^-$ cells into T cells. *J. Immunol.* 159: 694–702.

Downloaded from www.jimmunol.org on May 24, 2010

32. Lotzova, E., C. Savary, and R. Champlin. 1993. Genesis of human oncolytic natural killer cells from primitive $CD34^+CD33^-$ bone marrow progenitors. *J. Immunol.* 150: 5263–5269.
33. Miller, J., K. Alley, and P. McGlave. 1994. Differentiation of natural killer (NK) cells from human primitive marrow progenitors in a stroma-based long-term culture system: identification of a $CD34^+7^-$ NK progenitor. *Blood* 83: 2594–2601.
34. Ohteki, T., H. Yoshida, T. Matsuyama, G. S. Duncan, T. W. Mak, and P. S. Ohashi. 1998. The transcription factor interferon regulatory factor 1(IRF-1) is important during the maturation of natural killer 1.1^+ T cell receptor-α/β^+ ($NK1^+$ T) cells, natural killer cells, and intestinal intraepithelial T cells. *J. Exp. Med.* 187: 967–972.
35. Ogasawara, K., S. Hida, N. Azimi, Y. Tagaya, T. Sato, T. Yokochi-Fukuda, T. A. Waldmann, T. Taniguchi, and S. Taki. 1998. Requirement for IRF-1 in the microenvironment supporting development of natural killer cells. *Nature* 391: 700–703.
36. Lodolce, J. P., D. L. Boone, S. Chai, R. E. Swain, T. Dassopoulos, S. Trettin, and A. Ma. 1998. IL-15 receptor maintains lymphoid homeostasis by supporting lymphocyte homing and proliferation. *Immunity* 9: 669–676.
37. Suzuki, H., G. S. Duncan, H. Takimoto, and T. W. Mak. 1997. Abnormal development of intestinal intraepithelial lymphocytes and peripheral natural killer cells in mice lacking the IL-2 receptor β chain. *J. Exp. Med.* 185: 499–506.
38. Cao, X., E. W. Shores, J. Hu-Li, M. R. Anver, B. L. Kelsall, S. M. Russell, J. Drago, M. Noguchi, A. Grinberg, E. T. Bloom, et al. 1995. Defective lymphoid development in mice lacking expression of the common cytokine receptor γ chain. *Immunity* 2: 223–238.
39. DiSanto, J., W. Muller, D. Guy-Grand, A. Fischer, and K. Rajewsky. 1995. Lymphoid development in mice with a targeted deletion of the interleukin 2 receptor γ chain. *Proc. Natl. Acad. Sci. USA* 92: 377–381.
40. Spits, H. 2002. Development of $\alpha\beta$ T cells in the human thymus. *Nat. Rev. Immunol.* 2: 760–772.
41. Freud, A. G., A. Yokohama, B. Becknell, M. T. Lee, H. C. Mao, A. K. Ferketich, and M. A. Caligiuri. 2006. Evidence for discrete stages of human natural killer cell differentiation in vivo. *J. Exp. Med.* 203: 1033–1043.
42. Smyth, M. J., E. Cretney, J. M. Kelly, J. A. Westwood, S. E. A. Street, H. Yagita, K. Takeda, S. L. H. van Dommelen, M. A. Degli-Esposti, and Y. Hayakawa. 2005. Activation of NK cell cytotoxicity. *Mol. Immunol.* 42: 501–510.

Downloaded from www.jimmunol.org on May 24, 2010

Gain-of-function mutations and copy number increases of Notch2 in diffuse large B-cell lymphoma

Suk-young Lee,[1] Keiki Kumano,[1,2] Kumi Nakazaki,[2] Masashi Sanada,[1,2] Akihiko Matsumoto,[1] Go Yamamoto,[2] Yasuhito Nannya,[2] Ritsuro Suzuki,[3] Satoshi Ota,[4] Yasunori Ota,[5] Koji Izutsu,[2] Mamiko Sakata-Yanagimoto,[1,2,6] Akira Hangaishi,[2] Hideo Yagita,[7] Masashi Fukayama,[4] Masao Seto,[3] Mineo Kurokawa,[2] Seishi Ogawa[1,2,8] and Shigeru Chiba[1,6,9]

[1]Department of Cell Therapy and Transplantation Medicine, University of Tokyo Hospital, Tokyo 113-8655; [2]Department of Hematology and Oncology, Graduate School of Medicine, University of Tokyo, Tokyo 113-8655; [3]Division of Molecular Medicine, Aichi Cancer Center, Nagoya 464-8681; [4]Department of Pathology, Graduate School of Medicine, University of Tokyo, Tokyo 113-8655; [5]Department of Pathology, Toranomon Hospital, Tokyo 105-8470; [6]Department of Clinical and Experimental Hematology, Graduate School of Comprehensive Human Sciences, University of Tsukuba, Tsukuba 305-8575; [7]Department of Immunology, School of Medicine, Juntendo University, Tokyo 113-8431; [8]Core Research for Evolutional Science and Technology (CREST), Japan Science and Technology Agency, Tokyo, Japan 102-8655

(Received December 28, 2008/Revised January 22, 2009/Accepted January 22, 2009/Online publication March 25, 2009)

Signaling through the Notch1 receptor has a pivotal role in early thymocyte development. Gain of Notch1 function results in the development of T-cell acute lymphoblastic leukemia in a number of mouse experimental models, and activating *Notch1* mutations deregulate Notch1 signaling in the majority of human T-cell acute lymphoblastic leukemias. *Notch2*, another member of the *Notch* gene family, is preferentially expressed in mature B cells and is essential for marginal zone B-cell generation. Here, we report that 5 of 63 (~8%) diffuse large B-cell lymphomas, a subtype of mature B-cell lymphomas, have *Notch2* mutations. These mutations lead to partial or complete deletion of the proline-, glutamic acid-, serine- and threonine-rich (PEST) domain, or a single amino acid substitution at the C-terminus of Notch2 protein. Furthermore, high-density oligonucleotide microarray analysis revealed that some diffuse large B-cell lymphoma cases also have increased copies of the mutated *Notch2* allele. In the Notch activation-sensitive luciferase reporter assay *in vitro*, mutant Notch2 receptors show increased activity compared with wild-type Notch2. These findings implicate *Notch2* gain-of-function mutations in the pathogenesis of a subset of B-cell lymphomas, and suggest broader roles for *Notch* gene mutations in human cancers. (*Cancer Sci* 2009; 100: 920–926)

Signaling through the Notch receptor, triggered by the binding of ligands expressed on neighboring cells, has a key role in determining cell fate in a variety of cell lineages, including lymphocytes.[1,2] In mammals, there are four *Notch* genes that encode structurally similar single-pass and heterodimeric transmembrane receptors. Ligand binding initiates a series of intramolecular cleavages, which eventually liberates the intracellular domain of the transmembrane subunit of the intracellular Notch receptor (ICN). The ICN is then translocated to the nucleus and creates a transcriptional activating complex with RBP-Jκ, a constitutive DNA binding protein. During these processes, Notch proteins are intricately regulated by glycosylation, endocytosis, recycling, phosphorylation, and ubiquitylation before and after ICN liberation. Many of these regulatory processes appear to modify the biologic activity of Notch.[3] Notably, polyubiquitylation-based degradation is dependent on the proline-, glutamic acid-, serine- and threonine-rich (PEST) domain, located at the C-terminus of the Notch protein.

The physiologic roles of *Notch1* and *Notch2* have been clarified in mouse models, particularly in the lymphoid system. *Notch1* is preferentially expressed in immature T cells and is essential for specification of early hematopoietic progenitors toward the T cell fate and for early T cell development in the thymus.[4] In contrast, *Notch2* is preferentially expressed in mature B cells and is required for the generation of a mature B-cell subset, known as splenic marginal zone B (MZB) cells in mice.[5] *Notch1* was originally identified as a transforming gene in human T-cell acute lymphoblastic leukemia (T-ALL) cells harboring the t(7;9)(q34;q34) chromosomal translocation.[6] The N-terminal truncated form of Notch1 expressed in this type of T-ALL cell can induce the development of T-ALL when expressed in bone marrow cells that are then transplanted into recipient mice.[7] Importantly, more than 50% of childhood and 30–40% of adult human T-ALL cases carry *Notch1* mutations that lead to deregulated activation of Notch signaling,[8–11] indicating that accelerated Notch signaling contributes to the development of human neoplasms.

Two regions of the *Notch1* gene are major targets of oncogenic mutations in T-ALL. Missense, insertion, and deletion mutations in the heterodimerization domains are thought to decrease the stability of the dimer, consisting of the extracellular and transmembrane subunits, which results in the progression of Notch1 cleavage without ligand stimulation.[8,12] The other series of mutations accumulate in the PEST domain and its N-terminally flanking transactivation domain. All of these mutations cause partial or complete deletion of the PEST domain, considered to result in the prolonged half-life of Notch1 ICN, because the PEST domain is responsible for polyubiquitylation-based degradation of ICN.[13]

These lines of information about *Notch* genes led us to examine the possibility that deregulation of Notch2 signaling is involved in the development of mature B-cell lymphomas. We screened *Notch2* gene mutations at the heterodimerization and PEST domains in 109 B-cell lymphoma samples, and found mutations in five samples, all of which were diffuse large B-cell lymphomas (DLBCL). Interestingly, two of the five samples had an increased copy number of the mutated *Notch2* allele, and in another sample of the five, the total copy number of the *Notch2* allele was increased. Furthermore, we confirmed that the mutation-carrying Notch2 receptors had increased activity when stimulated by a ligand *in vitro*. We postulate that gain-of-function mutations of *Notch2* are involved in the pathogenesis of a subset of DLBCL.

Materials and Methods

Patient materials and genomic DNA preparation. Patients ($n = 109$) with various B-cell lymphomas were enrolled in the study after informed consent was obtained. The study design was approved by the ethics committees of the University of Tokyo (Tokyo, Japan) and Aichi Cancer Center (Nagoya, Japan). Genomic DNA

[9]To whom correspondence should be addressed. E-mail: schiba-tky@umin.net

doi: 10.1111/j.1349-7006.2009.01130.x
© 2009 Japanese Cancer Association

was extracted from cryopreserved samples using a commercial kit (Puregene; Gentra Systems, Minneapolis, MN, USA).

Polymerase chain reaction–single-stranded conformational polymorphism (PCR-SSCP). Based on the information of *Notch1* mutations in T-ALL and the high similarity between *Notch1* and *Notch2* genes, we confined our mutation analysis to exons 26, 27, and 34 of *Notch2* that correspond to the heterodimerization domains (exons 26 and 27) and the C-terminal region containing the transactivation and PEST domains (exon 34). Oligonucleotide primers designed to amplify whole exon 26 and exon 27, and five divided portions of exon 34 are listed in the Supporting Information (Table S1). The ^{32}P-labeled PCR product was subjected to SSCP analysis as described in published reports.[14] In brief, the PCR mixture was heated at 80°C and applied to 5% polyacrylamide gel containing 10% glycerol. After 2–4 h electrophoresis with cooling, the gel was dried on filter paper and exposed to X-ray film. The PCR products were directly sequenced or bands with aberrant migration were excised from the gel and subjected to direct sequencing when indicated.

High-density oligonucleotide microarray analysis. Genome-wide copy number detection analysis was carried out as described previously.[15] In brief, Affymetrix GeneChip Mapping 100K high-density oligonucleotide arrays (Affymetrix, Santa Clara, CA, USA) were used and the data were analyzed using the CNAG algorithm (Version 2.0. Genome Laboratory, University of Tokyo Hospital, Tokyo, Japan).

Fluorescence *in situ* hybridization. Bacterial artificial chromosome (BAC) clones RP11–723d17 (*Notch2*) and RP11–80d6 (1q23.3) were used to evaluate the copy number of the *Notch2* gene. BACs were obtained from the BAC/PAC Resource Center (Children's Hospital, Oakland, CA, USA). Fluorescence *in situ* hybridization experiments on interphase nuclei were carried out as described previously.[16]

Quantitative real-time PCR for genomic DNA. For the copy number evaluation of the *Notch2* gene by quantitative real-time PCR, genomic DNA was extracted from: samples L8 and W121672; a stomach cancer cell line (MKN45) that had a copy number loss at the *Notch2* (1p13) locus (data from microarray analysis not shown); and normal peripheral blood mononuclear cells. The *Notch2* gene dosage was measured using the primers: forward, TTCCCCAAGTGAGAGACATTT; and reverse, CAGACACTT-CACAGAACAGAA, and normalized by the relative DNA quantities measured by real-time PCR using the control locus (2q35) primers: forward, TGGCTGATGAACTTTTGCAC; and reverse, AGCGGTTGAGGTCTGTGAAC. Student's *t*-test was used for the statistical analysis.

Immunohistochemistry. Tissue sections were mounted on silanated slides, deparaffinized with xylene, rehydrated with a series of graded ethanols, processed with an autoclave in 10 mmol/L citrate buffer for 5 min, pH 6.0, treated with horse serum albumin to block non-specific staining, and immunostained. The detection of antibody binding was visualized by the avidin–biotin complex method using diaminobenzidine as the chromogen. The sections were counterstained with hematoxylin.

Plasmid preparation. In the human full-length Notch2 cDNA (wtN2) (a gift from S. Artavanis-Tsakonas, Harvard University, Cambridge, MA, USA), the stop codon corresponding to the nonsense mutation (7454 C/T), the single-base deletion mutation corresponding to 7120Del, and the point mutation corresponding to 7614 G/A were introduced. Mutant primers were used for PCR and the resulting products were sequenced and used to replace the corresponding fragment of wtN2 cDNA to create Notch2 with the nonsense mutation and the R2453Q mutation (nsmN2, delstN2, and rqN2, respectively). These cDNAs were inserted in pTracerCMV (Invitrogen, Carlsbad, CA, USA).

Establishment of CHO(r) cells stably expressing wild-type and mutant human Notch2. CHO(r) cells were transfected with pTracerCMV/wtN2, pTracerCMV/nsmN2, pTracerCMV/delstN2,

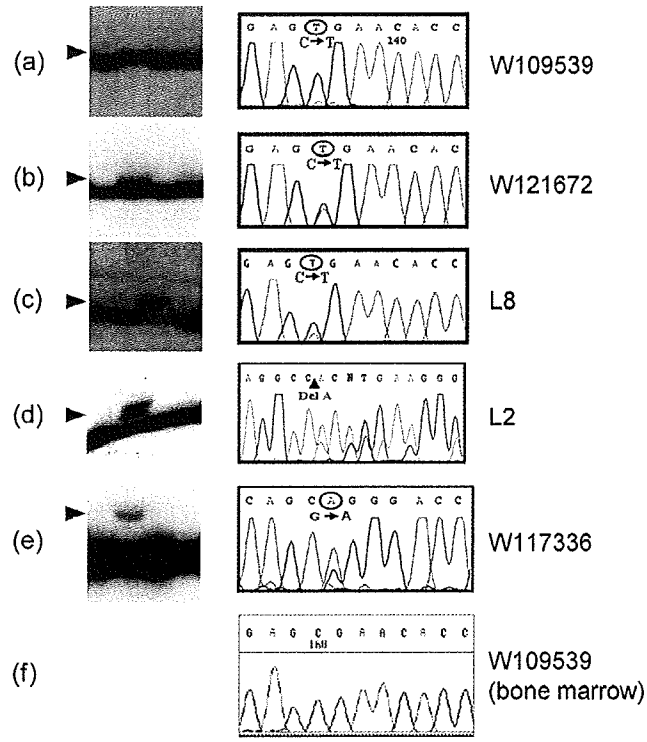

Fig. 1. Mutations of the *Notch2* gene in diffuse large B-cell lymphomas. Polymerase chain reaction–single-stranded conformational polymorphism and sequence analyses for samples having the nonsense mutation at 7454, C/T (W109539, W121672 and L8). Arrowheads indicate shifted bands. The shifted bands in (a) and (c) are obviously dominant against the normal band, suggesting the small amount of normal tissue contamination and unbalanced ratio of mutant and normal alleles. Those in (b) and (e) are minor compared with the normal band, suggesting the contamination of normal tissues, and those in (c) are comparable with the normal band. The shifted bands were excised from the gel and the extracted DNA was sequenced for samples W121672 and W117336. (f) Sequence of DNA prepared from the bone marrow cells obtained from the patient W109539.

and pTracerCMV/rqN2, and selected for zeocin (400 μg/mL) resistance. The resulting zeocin-resistant cells were single-cell sorted using the antihuman Notch2 monoclonal antibody (mAb). The antihuman Notch2 (MHN2-25, mouse IgG_{2a}) mAb was generated by immunizing BALB/c mice with human Notch2-Fc (the Fc portion of human IgG_1 was fused to the 22nd epidermal growth factor repeat of the extracellular region of human Notch2) and screening hybridomas producing mAbs specific for Notch2-Fc by enzyme-linked immunosorbent assay. MHN2-25 reacted with CHO(r) cells expressing human Notch2, as indicated by flow cytometry (Supporting Information Fig. S1).

Western blot analysis. Immunoblotting was carried out as described previously.[17] In brief, 1×10^6 wtN2/CHO(r), nsmN2/CHO(r), delstN2/CHO(r), and rqN2/CHO(r) cells were solubilized in 0.1 mL lysis buffer containing 1% NP-40, electrophoresed in 7.5% sodium dodecylsulfate polyacrylamide gel, transferred onto Immobilon-P membrane (Millipore, Billerica, MA, USA). It was then probed with a mAb recognizing the intracellular domain of human and murine Notch2 (C651.6DbHN; Developmental Studies Hybridoma Bank, University of Iowa, Iowa City, IA, USA) and an alkaline phosphatase-conjugated secondary antibody (Promega, Madison, WI, USA).

Transcriptional activation assay. The luciferase assay was carried out as described previously.[17] In brief, 2×10^5 CHO(r) cells expressing wtN2, Notch2 with truncatation at 2400 (nsmN2),

© 2009 Japanese Cancer Association

Table 1. *Notch2* mutational status in five patients with diffuse large B-cell lymphoma

Sample	Nucleic acid change	Amino acid change	Copy number	Immunohistochemistry		
				CD10	BCL6	MUM-1
W109539	7454 C/T	2400 Stop	Multiple	–	+	+
W121672	7454 C/T	2400 Stop	3	–	+	+
L8	7454 C/T	2400 Stop	2†	–	+	+
L2	7120 Del A	2288PLKGSTStop	NA	–	+	+
W117336	7614 G/A	2453 R/Q	2	–	+	+

†Uniparental disomy for the mutated *Notch2* allele is indicated. NA, information not available.

Table 2. Characteristics of five patients with diffuse large B-cell lymphoma who had *Notch2* mutations

Patient	Age/sex	CS/IPI	Treatment/Response	Survival	Others
W109539	64/M	IIIA/LI	R-CHOP/CRu/relapse	1.6 y (d1)	Acromegaly, DM, AAA (postoperation)
W121672	71/M	NA	NA	NA	–
L8	66/M	IVA/NA	NA	NA	–
L2	61/F	IV/NA	CHOP/CR	7 y (alive)	BCL2 rearrangement
W117336	83/F	IIIA/LI	RT, CHOP	0.3 y (d2)	–

AAA, abdominal aortic aneurysm; CHOP, cyclophosphamide, adriamycin, vincristine and predonisolon; CR, complete remission; CRu, complete remission uncertain; CS, clinical stage; d1, died of advanced lymphoma; d2, died of advanced lymphoma after first chemotherapy; DM, diabetes mellitus; F, female; IPI, international prognostic index; LI, low intermediate; M, male; NA, information not available; R-CHOP, rituximab plus CHOP, with 4-0-tetrahydropyranyl-adriamycin instead of adriamycin, four courses; RT, radiation therapy; y, years.

Notch2 with truncation after 6 amino acids insertion at 2288 (delstN2), and Notch2 with an R2453Q mutation (rqN2) were inoculoated in a 6-well dish and the next day transfected with the pGa981-6 luciferase reporter plasmid (2 μg) using the Superfect transfection reagent (Qiagen, Hilden, Germany). The β-galactosidase-expressing plasmid, pCMV/β-Gal (0.2 μg) was cotransfected when indicated. The cells were harvested after 3 h, suspended in 3 mL medium, and a 200 μL aliquot was replated in a 48-well dish coated with soluble human Delta1 (Delta1-Fc, a chimeric protein composed of the extracellular domain of human Delta1 and the Fc portion of human IgG,[18,19] a gift from S. Sakano, Asahi Kasei, Tokyo, Japan). After 24 h incubation, the cellular extracts were used to measure luciferase and, when applied, β-galactosidase activities. Two independent clones were used to compare the luciferase activity of each Notch2 protein and bulk transfectants were used to evaluate the effect of N-[N-(3,5-difluorophenacetyl)-L-alanyl]-S-phenylglycine t-butyl ester (DAPT; Calbiochem, San Diego, CA, US), a γ-secretase inhibitor.

Results

***Notch2* gene is mutated in a subset of DLBCL.** *Notch2* gene mutations were screened in 109 B-cell lymphoma samples, including 63 DLBCLs, 18 follicular lymphomas, and 28 MZB-cell lymphomas or mucosa-associated lymphoid tissue lymphomas. Exons 26 and 27, encoding the N- and C-terminal heterodimerization domains, and a portion of exon 34, encoding the PEST domain and its bilateral flanking regions, were amplified by PCR using genomic DNA with the primers listed in the Supporting Information (Table S1) and examined for mutations using the PCR-SSCP method.[20]

Five distinct nucleotide changes were detected in 11 of the 109 B-cell lymphoma samples, exclusively in exon 34. Whereas two of the five changes detected in 6 of the 11 samples were single nucleotide polymorphisms (SNP) without amino acid changes, the other three nucleotide changes detected in the remaining 5 samples (Fig. 1a–e) were thought to represent somatic mutations resulting in premature truncation or single amino acid substitution (Table 1). A nonsense mutation, C to T at nucleotide 7454 (based on the published human *Notch2* sequence, NM_024408), in three cases (Fig. 1a–c) and a single-base deletion at position 7120 in another case (Fig. 1d), led to premature truncation of the Notch2 protein (Table 1). These Notch2 proteins lacked a part or the entire region of the PEST domain. The other single nucleotide change, G to A at 7614, resulted in the replacement of arginine with glutamine on the C-terminal side of the PEST domain (Fig. 1e and Table 1). The G7614A change is not listed in the public SNP database (http://www.ncbi.nlm.nih.gov/projects/SNP/; as of October 23, 2007). In addition, the dose of the mutant A allele was unbalanced relative to the wild-type G allele (Fig. 1e), further decreasing the possibility of an SNP. Constitutive DNA was available in one case (W109539) and was confirmed to be the wild-type sequence (Fig. 1f), which definitely concluded that the mutation in the tumor was of somatic origin. Clinical information of the five patients is summarized in Table 2.

Mutation-carrying cases show same expression pattern of CD10, BCL6, and MUM-1. All five cases with *Notch2* mutations were diagnosed as DLBCL, and were uniformly immunohistochemically negative for CD10 and positive for BCL6 and MUM-1 (Fig. 2). We have reviewed 24 DLBCL subjects without *Notch2* mutations for expression of CD10, BCL6 and MUM-1. The immunohistochemistry study revealed that CD10, BCL6, and MUM-1 were positive in 4, 19, and 16 subjects, respectively. Among these, the CD10-negative, BCL6-positive, and MUM-1-positive staining pattern was seen in 10 (data not shown). Thus, this pattern was seen in five out of five *Notch2* mutation-carrying subjects and 10 out of 24 *Notch2* mutation-negative subjects, making the comparison statistically significant ($P = 0.042$; Fisher's exact test). This estimation is consistent with the previous report[21] and indicates that CD10-negative, BCL6-positive, and MUM-1-positive DLBCL might represent a fraction of non-germinal center B-cell-like (non-GCB)-DLBCL, according to the immunohistochemistry-based DLBCL subclassification.[21] DLBCL cases carrying the gain-of-function type *Notch2* mutations, thus, might constitute a discrete subset of non-GCB-DLBCL.

doi: 10.1111/j.1349-7006.2009.01130.x
© 2009 Japanese Cancer Association

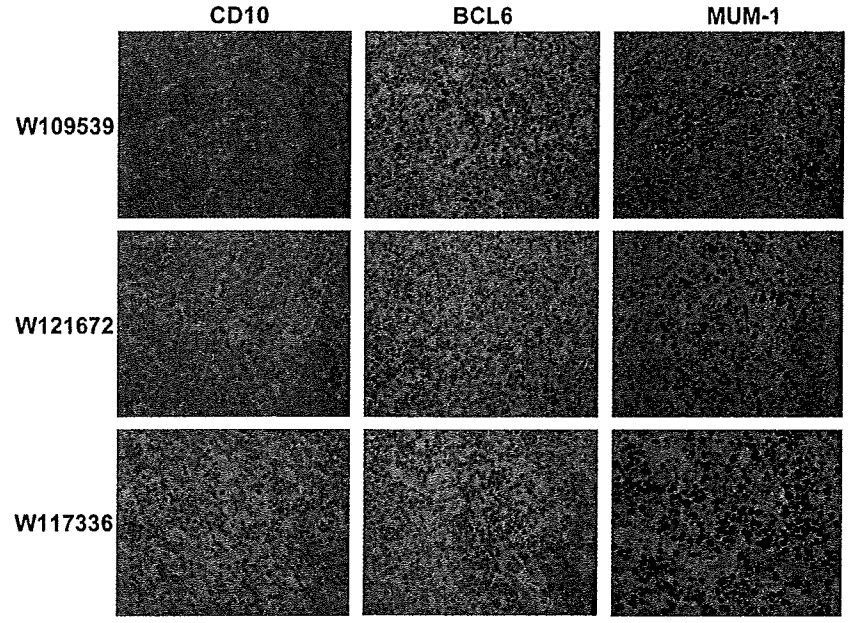

Fig. 2. Immunohistochemical staining of lymphoma specimens for CD10, BCL6, and MUM-1. Antibodies used were anti-CD10 monoclonal antibody (mAb) (56C6; Novocastra, Norwell, MA, USA), anti-BCL6 mAb (P1F6; Novocastra), and antihuman MUM-1 mAb (MUM1p; Dako, Glostrup, Denmark). The detection of antibody binding was visualized by the avidin–biotin complex method using diaminobenzidine as the chromogen. An Elipse 80i microscope was used (Nikon, Tokyo, Japan); original magnification, × 200. Camera, Dxm1200F (Nikon). Acquisition software, Act-1 (Nikon).

Some mutation-carrying samples have increased copy number of mutated Notch2 allele. Of particular interest is the fact that some oncogenic mutations are associated with increases in DNA copy number.[22,23] A high-density oligonucleotide microarray analysis[15] was carried out for 35 of 63 DLBCL samples in the current cohort to evaluate genome-wide copy number alterations. This analysis revealed an increased copy number of the *Notch2* allele in two samples, both of which carried the nonsense mutation. The other 33 samples did not show *Notch2* copy number alterations. In one sample (W109539), amplification of the *Notch2* locus in chromosome 1p was indicated by microarray (Fig. 3a, left panel) and fluorescence *in situ* hybridization (Fig. 3b) analyses. An allele-specific copy number detection analysis revealed an increase in the copy number of a single *Notch2* allele (Fig. 3a, left panel). This allele must correspond to the allele carrying the mutated *Notch2* gene because the mutated band was overwhelmingly dominant in the PCR-SSCP analysis (Fig. 1a). In the other sample (W121672) with a *Notch2* copy number increase, the genomic region encompassing the *Notch2* locus on chromosome 1p through the telomere of chromosome 1q had three copies, whereas most of the 1p region had only one copy (Fig. 3a, right panel). The *Notch2* copy number increase was confirmed by a quantitative real-time PCR analysis (Fig. 3c). We were unable to determine whether the third *Notch2* allele contained wild-type or mutant *Notch2* in this sample. In the third sample carrying the nonsense mutation (L8), a change in the *Notch2* copy number was not detected in the microarray analysis (data not shown) and quantitative PCR analysis revealed that the copy number was normal (Fig. 3c). Both *Notch2* alleles in this sample, however, were likely to have the nonsense mutation, thus representing uniparental disomy, losing the wild-type *Notch2*, because the mutant band was overwhelmingly dominant in the PCR-SSCP analysis (Fig. 1c). Taken together, these findings indicate that some DLBCL samples have *Notch2* mutations and an increased copy number of the mutated *Notch2* gene.

***Notch2* receptors with mutations have increased activity *in vitro*.** To investigate the function of the Notch2 receptors encoded by mRNA with the nonsense mutation (nsmN2), the single-base deletion mutation (delstN2), and missense mutation (rqN2), we established CHO(r) cell lines[17] expressing wild-type Notch2, nsmN2, delstN2, and rqN2 [wtN2/CHO(r), nsmN2/CHO(r), delstN2/CHO(r), and rqN2/CHO(r)] and obtained independent clones expressing each Notch2 protein at similar levels, using fluorescence-activated cell sorting with human Notch2-specific antibody (Fig. 4a; Supporting Information Fig. S1). A Western blot analysis showed that the expected sizes of the transmembrane subunit species were expressed at comparable levels (Fig. 4b). In a Notch-sensitive luciferase reporter assay,[24] the luciferase activity was significantly increased in nsmN2/CHO(r), delstN2/CHO(r), and rqN2/CHO(r) cells, compared with that in wtN2/CHO(r) cells when stimulated with Delta1-Fc. Basal luciferase activities with control IgG also tended to be higher in the three mutant Notch2-expressing CHO(r) cells lines than in wtN2/CHO(r) (Fig. 4c). These results indicated that all three kinds of mutation-carrying Notch2 had significantly increased levels of transcriptional activity compared with wtN2, irrespective of the strength of the Delta1 stimulation.

To evaluate the effect of γ-secretase inhibitor on wtN2 and nsmN2, we added graded concentrations of DAPT to the Delta1-Fc-stimulated bulk wtN2/CHO(r) and nsmN2/CHO(r). The elevated luciferase activity was reproducible with the bulk nsmN2/CHO(r), which was reduced by DAPT in a concentration-dependent manner (Fig. 4d). The luciferase levels of both wtN2/CHO(r) and nsmN2/CHO(r) at 3 μM DAPT in the presence of Delta1-Fc were below those in the presence of control IgG without DAPT, implying spontaneous Notch2 activity with only IgG in the culture system. The results also indicate that increased Notch2 activity by the PEST domain deletion is still dependent on γ-secretase activity.

Discussion

The results of the present study showed gain-of-function mutations of *Notch2* and increased copy numbers of the mutated *Notch2* allele in a subset of DLBCL. Both nonsense mutations and single-base deletion mutations that we found in *Notch2* cause partial or complete deletion of the Notch2 PEST domain. Given the marked structural similarities between Notch1 and Notch2, these mutations are thought to prolong the half-life of Notch2 ICN. In some T-ALL cell lines, both heterodimerization and PEST domain mutations lie in *cis* in the same *Notch1* allele. The reporter transcriptional activity of Notch1 with these double mutations was remarkably higher than that of wild-type Notch1 and Notch1 with a single mutation at either the heterodimerization

© 2009 Japanese Cancer Association

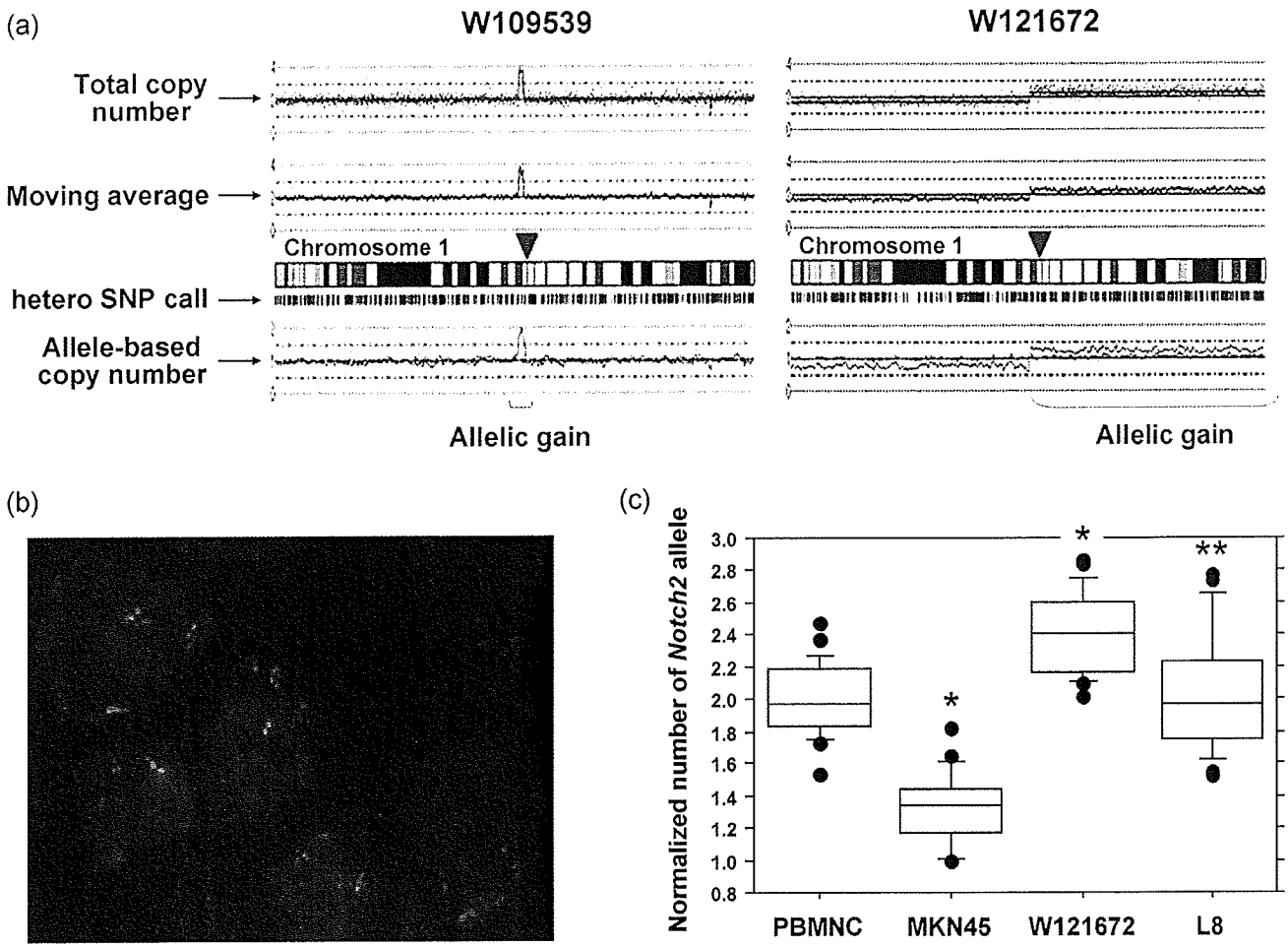

Fig. 3. Copy number increases of mutated Notch2 allele in diffuse large B-cell lymphomas. (a) High-density oligonucleotide microarray analysis using the CNAG program (CREST, Japan Science and Technology Agency, Tokyo, Japan) for samples W109539 and W121672. The copy number of the *Notch2*-encompassing allele is greatly increased in W109539 and mildly increased in W121672. Red arrow, centromere. hetero, heterozygous; SNP, single nucleotide polymorphism. (b) Fluorescence *in situ* hybridization analysis for sample W109539 using probes corresponding to *Notch2* (green signals) and a reference sequence on 1q23.3 (red signals). (c) Copy number evaluation of the *Notch2* gene by quantitative real-time polymerase chain reaction for samples L8 and W121672. The quantity of genomic DNA, extracted from samples L8 and W121672, MKN45 [a stomach cancer cell line having a copy number loss at the *Notch2* (1p13) locus], and normal peripheral blood mononuclear cells (PBMNC), was normalized by real-time reverse transcription–polymerase chain reaction for the control locus (2q35). Statistical analysis (Student's *t*-test) showed that the *Notch2* gene dose was unchanged in sample L8, and significantly increased in sample W121782, relative to the *Notch2* gene dose in the PBMNC, whose mean level was adjusted to two copies. The number of samples was 24 in each arm. $*P < 0.0001$; $**P = 0.79$.

or PEST domain in the absence of exogenous ligand stimulation. The activity of Notch1 with a PEST domain deletion mutation alone was only marginally higher than that of wild-type Notch1[8]. We did not detect mutations in either heterodimerization domain of Notch2 in the current cohort. It might be possible to identify those mutations if the number of samples is increased. With the PEST domain deletion alone, however, nsmN2 had a highly significant increase in activity compared with wtN2. Thus, there appears to be some disagreement between the effects of Notch1 PEST domain deletion and Notch2 PEST domain deletion, although difference in the experimental systems used in the two studies might cause such apparent disagreement. It remains to be determined whether similar mutations found in Notch1 and Notch2 have different biochemical and biologic significance.

The activity was also increased in rqN2, which has the 2453R/Q single amino acid substitution. This amino acid is located on the C-terminal side of the PEST domain, and it is not known whether this change affects the structure or function of the PEST domain. Nevertheless, as the arginine residue is often a target of protein modification such as methylation,[25,26] this amino acid change might convey a significant alteration in the protein function and be involved in lymphomagenesis.

There are other examples of copy number increases associated with oncogenic gene alterations, such as double Philadelphia chromosomes (*BCR/ABL* copy number increase) in the blastic crisis of chronic myelogenous leukemia[27] and homozygous *JAK2* mutations in polycythemia vera,[22,23] both of which represent clonal evolution and selection. In the present study, we showed that at least two (or possibly three) cases had increased copy numbers of the mutated *Notch2* allele due to gene amplification or mitotic recombination. This finding agrees with the recent understanding that the allelic copy number increase after an oncogenic mutation is a common mechanism of further transformation and selection of neoplastic cells.

Whether the presence of *Notch2* gain-of-function mutations has a prognostic indicator or further define a clinical entity within DLBCL is yet to be clarified. Although the number of cases is still small, our finding that all five cases with *Notch2*

doi: 10.1111/j.1349-7006.2009.01130.x
© 2009 Japanese Cancer Association

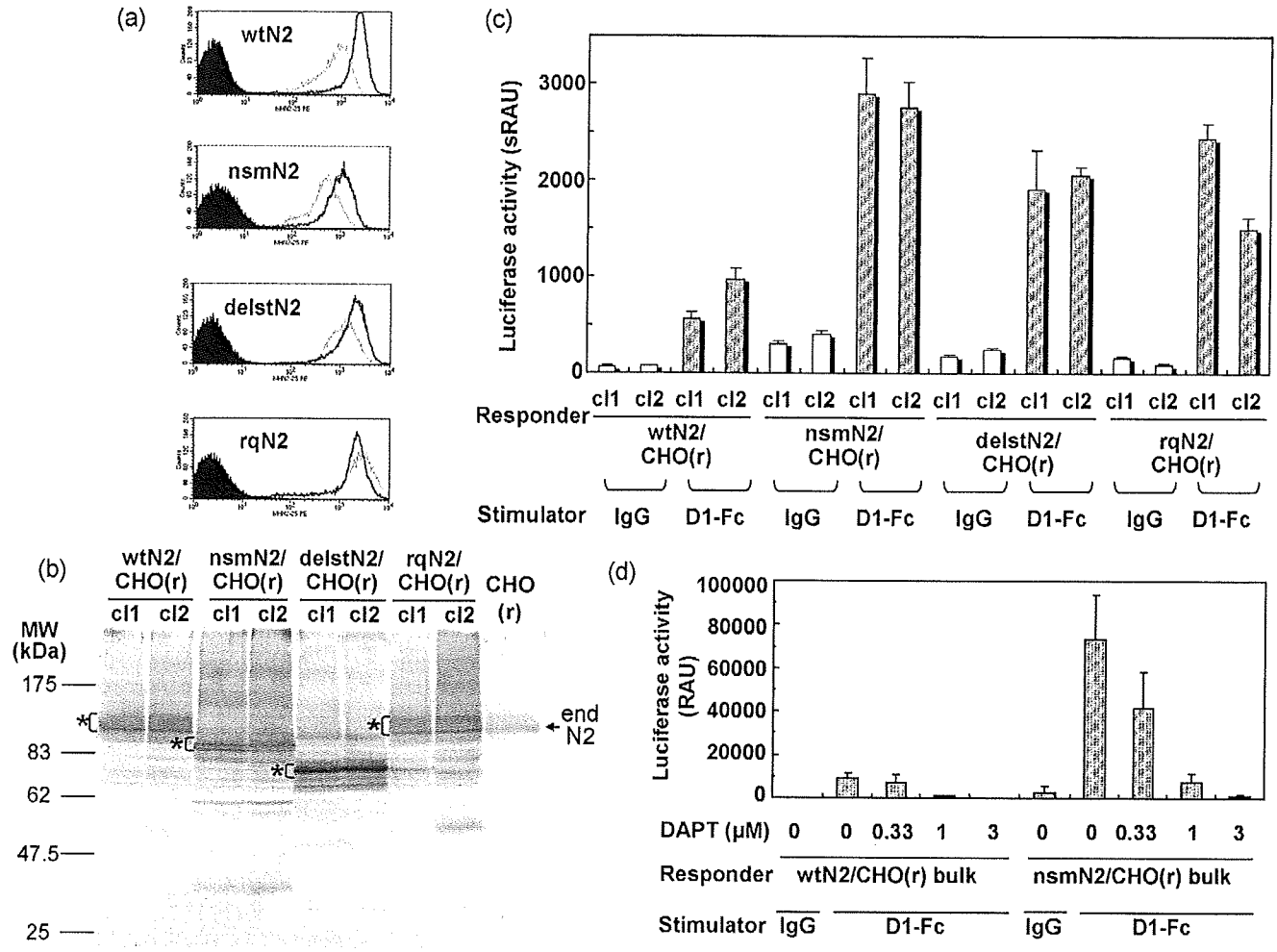

Fig. 4. Functional analysis of human full-length Notch2 cDNA (wtN2), and Notch2 with the nonsense mutation (nsmN2), single-base deletion mutation (delstN2), or R2453Q mutation (rqN2). (a) Flow cytometric analysis of CHO(r) clones expressing wtN2, nsmN2, delstN2, and rqN2 at similar expression levels. Each clone (cl1 and cl2 represented by green and red lines, respectively) of wtN2/CHO(r), nsmN2/CHO(r), delstN2/CHO(r), and rqN2/CHO(r) was analyzed by flow cytometry using the antihuman Notch2 antibody MHN2-25. Purple curves represent isotype control. (b) Western blot analysis of CHO(r) clones expressing wtN2, nsmN2, delstN2, and rqN2 using an antibody recognizing the intracellular domain of Notch2. Asterisks indicate the transmembrane species of each Notch2 protein. MW, molecular weight. (c) Reporter gene transactivation by wtN2, nsmN2, delstN2, and rqN2. Each clone (cl1 and cl2) was cultured in a dish coated with human Delta1-Fc (D1-Fc) or control IgG. Data are means of quadricate experiments. Error bars represent standard deviations. A representative experiment from repeated experiments is shown. sRAU, relative arbitrary units standardized by β-galctosidase activity. (d) Inhibition of luciferase activity by N-[N-(3,5-difluorophenacetyl)-L-alanyl]-S-phenylglycine t-butyl ester (DAPT), a γ-secretase inhibitor. Bulk CHO(r) cells transfected with wtN2 or nsmN2 were stimulated with D1-Fc or control IgG with graded concentrations of DAPT. RAU, relative arbitrary units.

mutations showed the same immunohistochemical staining pattern for CD10, BCL6 and MUM-1 might provide insight into this issue. DLBCL is highly heterogeneous clinically, morphologically, and genetically. The tissue microarray study based on immunostaining of the tissue samples identified three antigens (CD10, BCL6 and MUM-1) as useful markers to predict the results of mRNA expression array studies[28–30] and the staining pattern of these three antigens could be used to divide DLBCL cases into GCB and non-GCB groups.[21] Whereas all the five cases carrying *Notch2* mutations in our study belonged to the non-GCB group of DLBCL in this criterion, Troen *et al.* recently reported *Notch2* mutations in two cases of MZB-cell lymphomas.[31] Positions of these mutations are different from those that we found, and their effect on the Notch2 function is not shown. We did not find *Notch2* mutations in MZB-cell lymphomas in our cohort, yet the number of samples was not sufficient to draw conclusions. Although we were unable to find evidence that some or all the five cases carrying *Notch2* mutations in our cohort are DLBCL transformed from MZB-cell lymphoma, this might be an interesting possibility.

Enhanced activation of Notch signaling by exogenous ligand stimulation or expression of constitutively active Notch proteins supports the growth of a variety of tumor cells, including chronic lymphocytic leukemia,[32] non-Hodgkin's lymphoma, and multiple myeloma[33] cells. Alternatively, inhibition of Notch signaling by γ-secretase inhibitors suppresses the growth of those tumor cells, in which enhanced Notch signaling might be involved in tumorigenesis.[34] In contrast, a study of mice with a *Notch1* deletion in keratinocytes revealed the tumor-suppressive feature of Notch signaling.[35] In a similar context, Notch2 activation induces growth suppression in a wide range of B-cell malignancies, raising the possibility that Notch2 functions as a tumor suppressor in B cells.[36] Thus, there appears to be a controversy regarding whether Notch signaling has an oncogenic or antioncogenic role in mature B-cell malignancies. It might be possible that Notch signaling can induce both growth suppression and tumor promo-

© 2009 Japanese Cancer Association

tion in the B-cell compartment, depending on the target window within the various developmental stages of B cells.

Although it will require additional studies, including development of animal models, to draw a definitive conclusion about the role of Notch2 mutations in lymphomagenesis, our observations in this study strongly indicate that deregulation of Notch2 signaling by somatic *Notch2* gene abnormalities contributes to the development of a subset of DLBCL, the most frequent type of non-Hodgkin's lymphoma. Developing inhibitors of individual Notch molecules might provide a new strategy for the treatment of different kinds of malignancies, including T-ALL and DLBCL.

Acknowledgments

We thank Dr S. Sakano (Asahi Kasei) for the human Delta1 cDNA, Dr S. Shirahata (Kyushu University) for CHO(r), Dr S. Artavanis-Tsakonas (Harvard University) for the human full-length Notch2 cDNA, and Dr A. Harashima (Hayashibara Biomedical Institute) for the cell lines. We are grateful for the support provided by Dr M. Kato (University of Tokyo) and technical assistance by Y. Mori. Financial support was provided by Grants-in-Aid for Scientific Research from the Ministry of Education, Culture, Sports, Science, and Technology of Japan (KAKENHI #18013012 and #19390258), and grants from the Sagawa Foundation for the Promotion of Cancer Research and Osaka Cancer Foundation (SC).

References

1 Chiba S. Notch signaling in stem cell systems. *Stem Cells* 2006; **24**: 2437–47.
2 Wilson A, Radtke F. Multiple functions of Notch signaling in self-renewing organs and cancer. *FEBS Lett* 2006; **580**: 2860–8.
3 Bray SJ. Notch signalling: a simple pathway becomes complex. *Nat Rev Mol Cell Biol* 2006; **7**: 678–89.
4 Radtke F, Wilson A, Stark G *et al.* Deficient T cell fate specification in mice with an induced inactivation of Notch1. *Immunity* 1999; **10**: 547–58.
5 Saito T, Chiba S, Ichikawa M *et al.* Notch2 is preferentially expressed in mature B cells and indispensable for marginal zone B lineage development. *Immunity* 2003; **18**: 675–85.
6 Ellisen LW, Bird J, West DC *et al.* TAN-1, the human homolog of the Drosophila notch gene, is broken by chromosomal translocations in T lymphoblastic neoplasms. *Cell* 1991; **66**: 649–61.
7 Pear WS, Aster JC, Scott ML *et al.* Exclusive development of T cell neoplasms in mice transplanted with bone marrow expressing activated Notch alleles. *J Exp Med* 1996; **183**: 2283–91.
8 Weng AP, Ferrando AA, Lee W *et al.* Activating mutations of NOTCH1 in human T cell acute lymphoblastic leukemia. *Science* 2004; **306**: 269–71.
9 Lee SY, Kumano K, Masuda S *et al.* Mutations of the Notch1 gene in T-cell acute lymphoblastic leukemia: analysis in adults and children. *Leukemia* 2005; **19**: 1841–3.
10 Zhu YM, Zhao WL, Fu JF *et al.* NOTCH1 mutations in T-cell acute lymphoblastic leukemia: prognostic significance and implication in multifactorial leukemogenesis. *Clin Cancer Res* 2006; **12**: 3043–9.
11 Breit S, Stanulla M, Flohr T *et al.* Activating NOTCH1 mutations predict favorable early treatment response and long-term outcome in childhood precursor T-cell lymphoblastic leukemia. *Blood* 2006; **108**: 1151–7.
12 Sanchez-Irizarry C, Carpenter AC, Weng AP, Pear WS, Aster JC, Blacklow SC. Notch subunit heterodimerization and prevention of ligand-independent proteolytic activation depend, respectively, on a novel domain and the LNR repeats. *Mol Cell Biol* 2004; **24**: 9265–73.
13 Oberg C, Li J, Pauley A, Wolf E, Gurney M, Lendahl U. The Notch intracellular domain is ubiquitinated and negatively regulated by the mammalian Sel-10 homolog. *J Biol Chem* 2001; **276**: 35847–53.
14 Murakami Y, Hayashi K, Hirohashi S, Sekiya T. Aberrations of the tumor suppressor p53 and retinoblastoma genes in human hepatocellular carcinomas. *Cancer Res* 1991; **51**: 5520–5.
15 Nannya Y, Sanada M, Nakazaki K *et al.* A robust algorithm for copy number detection using high-density oligonucleotide single nucleotide polymorphism genotyping arrays. *Cancer Res* 2005; **65**: 6071–9.
16 Wang L, Ogawa S, Hangaishi A *et al.* Molecular characterization of the recurrent unbalanced translocation der (1;7) (q10;p10). *Blood* 2003; **102**: 2597–604.
17 Shimizu K, Chiba S, Kumano K *et al.* Mouse jagged1 physically interacts with notch2 and other notch receptors. Assessment by quantitative methods. *J Biol Chem* 1999; **274**: 32961–9.
18 Karanu FN, Murdoch B, Miyabayashi T *et al.* Human homologues of Delta-1 and Delta-4 function as mitogenic regulators of primitive human hematopoietic cells. *Blood* 2001; **97**: 1960–7.
19 Suzuki T, Yokoyama Y, Kumano K *et al.* Highly efficient *ex vivo* expansion of human hematopoietic stem cells using Delta1-Fc chimeric protein. *Stem Cells* 2006; **24**: 2456–65.
20 Hangaishi A, Ogawa S, Imamura N *et al.* Inactivation of multiple tumor-suppressor genes involved in negative regulation of the cell cycle, MTS1/p16INK4A/CDKN2, MTS2/p15INK4B, p53, and Rb genes in primary lymphoid malignancies. *Blood* 1996; **87**: 4949–58.
21 Hans CP, Weisenburger DD, Greiner TC *et al.* Confirmation of the molecular classification of diffuse large B-cell lymphoma by immunohistochemistry using a tissue microarray. *Blood* 2004; **103**: 275–82.
22 James C, Ugo V, Le Couedic JP *et al.* A unique clonal JAK2 mutation leading to constitutive signalling causes polycythaemia vera. *Nature* 2005; **434**: 1144–8.
23 Kralovics R, Passamonti F, Buser AS *et al.* A gain-of-function mutation of JAK2 in myeloproliferative disorders. *N Engl J Med* 2005; **352**: 1779–90.
24 Shimizu K, Chiba S, Hosoya N *et al.* Binding of Delta1, Jagged1, and Jagged2 to Notch2 rapidly induces cleavage, nuclear translocation, and hyperphosphorylation of Notch2. *Mol Cell Biol* 2000; **20**: 6913–22.
25 Bedford MT, Richard S. Arginine methylation an emerging regulator of protein function. *Mol Cell* 2005; **18**: 263–72.
26 Blanchet F, Cardona A, Letimier FA, Hershfield MS, Acuto O. CD28 costimulatory signal induces protein arginine methylation in T cells. *J Exp Med* 2005; **202**: 371–7.
27 Avanzi GC, Giovinazzo B, Saglio G *et al.* Duplication of Ph and of $9q^+$ chromosomes during the blastic transformation of a CML case. *Cancer Genet Cytogenet* 1987; **29**: 57–63.
28 Alizadeh AA, Eisen MB, Davis RE *et al.* Distinct types of diffuse large B-cell lymphoma identified by gene expression profiling. *Nature* 2000; **403**: 503–11.
29 Shipp MA, Ross KN, Tamayo P *et al.* Diffuse large B-cell lymphoma outcome prediction by gene-expression profiling and supervised machine learning. *Nat Med* 2002; **8**: 68–74.
30 Rosenwald A, Wright G, Chan WC *et al.* The use of molecular profiling to predict survival after chemotherapy for diffuse large-B-cell lymphoma. *N Engl J Med* 2002; **346**: 1937–47.
31 Troen G, Wlodarska I, Warsame A, Hernandez Llodra S, De Wolf-Peeters C, Delabie J. NOTCH2 mutations in marginal zone lymphoma. *Haematologica* 2008; **93**: 1107–9.
32 Hubmann R, Schwarzmeier JD, Shehata M *et al.* Notch2 is involved in the overexpression of CD23 in B-cell chronic lymphocytic leukemia. *Blood* 2002; **99**: 3742–7.
33 Jundt F, Probsting KS, Anagnostopoulos I *et al.* Jagged1-induced Notch signaling drives proliferation of multiple myeloma cells. *Blood* 2004; **103**: 3511–15.
34 Leong KG, Karsan A. Recent insights into the role of Notch signaling in tumorigenesis. *Blood* 2006; **107**: 2223–33.
35 Nicolas M, Wolfer A, Raj K *et al.* Notch1 functions as a tumor suppressor in mouse skin. *Nat Genet* 2003; **33**: 416–21.
36 Zweidler-McKay PA, He Y, Xu L *et al.* Notch signaling is a potent inducer of growth arrest and apoptosis in a wide range of B-cell malignancies. *Blood* 2005; **106**: 3898–906.

Supporting Information

Additional Supporting Information may be found in the online version of this article:

Fig. S1. Specific binding of the mouse antihuman Notch2 monoclonal antibody (MHN2-25). MHN2-25 was added to individual CHO(r) cells and analyzed by fluorescence-activated cell sorting. CHO(r), parental CHO(r); wtN1/CHO(r), CHO(r) cells stably transfected with pTracerCMV/wild-type human Notch1; wtN2/CHO(r), CHO(r) cells stably transfected with pTracerCMV/wild-type human Notch2. Broken lines, biotin-conjugated mouse IgG2a/k (isotype control); solid lines, biotin-conjugated MHN2-25.

Table S1. Primers for polymerase chain reaction–single-stranded conformational polymorphism

Please note: Wiley-Blackwell are not responsible for the content or functionality of any supporting materials supplied by the authors. Any queries (other than missing material) should be directed to the corresponding author for the article.

doi: 10.1111/j.1349-7006.2009.01130.x
© 2009 Japanese Cancer Association

nature

Vol 459|4 June 2009|doi:10.1038/nature07969

LETTERS

Frequent inactivation of A20 in B-cell lymphomas

Motohiro Kato[1,2], Masashi Sanada[1,5], Itaru Kato[6], Yasuharu Sato[7], Junko Takita[1,2,3], Kengo Takeuchi[8], Akira Niwa[6], Yuyan Chen[1,2], Kumi Nakazaki[1,4,5], Junko Nomoto[9], Yoshitaka Asakura[9], Satsuki Muto[1], Azusa Tamura[1], Mitsuru Iio[1], Yoshiki Akatsuka[11], Yasuhide Hayashi[12], Hiraku Mori[13], Takashi Igarashi[2], Mineo Kurokawa[4], Shigeru Chiba[3], Shigeo Mori[14], Yuichi Ishikawa[8], Koji Okamoto[10], Kensei Tobinai[9], Hitoshi Nakagama[10], Tatsutoshi Nakahata[6], Tadashi Yoshino[7], Yukio Kobayashi[9] & Seishi Ogawa[1,5]

A20 is a negative regulator of the NF-κB pathway and was initially identified as being rapidly induced after tumour-necrosis factor-α stimulation[1]. It has a pivotal role in regulation of the immune response and prevents excessive activation of NF-κB in response to a variety of external stimuli[2–7]; recent genetic studies have disclosed putative associations of polymorphic *A20* (also called *TNFAIP3*) alleles with autoimmune disease risk[8,9]. However, the involvement of A20 in the development of human cancers is unknown. Here we show, using a genome-wide analysis of genetic lesions in 238 B-cell lymphomas, that *A20* is a common genetic target in B-lineage lymphomas. A20 is frequently inactivated by somatic mutations and/or deletions in mucosa-associated tissue lymphoma (18 out of 87; 21.8%) and Hodgkin's lymphoma of nodular sclerosis histology (5 out of 15; 33.3%), and, to a lesser extent, in other B-lineage lymphomas. When re-expressed in a lymphoma-derived cell line with no functional *A20* alleles, wild-type A20, but not mutant A20, resulted in suppression of cell growth and induction of apoptosis, accompanied by downregulation of NF-κB activation. The A20-deficient cells stably generated tumours in immunodeficient mice, whereas the tumorigenicity was effectively suppressed by re-expression of A20. In A20-deficient cells, suppression of both cell growth and NF-κB activity due to re-expression of A20 depended, at least partly, on cell-surface-receptor signalling, including the tumour-necrosis factor receptor. Considering the physiological function of A20 in the negative modulation of NF-κB activation induced by multiple upstream stimuli, our findings indicate that uncontrolled signalling of NF-κB caused by loss of A20 function is involved in the pathogenesis of subsets of B-lineage lymphomas.

Malignant lymphomas of B-cell lineages are mature lymphoid neoplasms that arise from various lymphoid tissues[10,11]. To obtain a comprehensive registry of genetic lesions in B-lineage lymphomas, we performed a single nucleotide polymorphism (SNP) array analysis of 238 primary B-cell lymphoma specimens of different histologies, including 64 samples of diffuse large B-cell lymphomas (DLBCLs), 52 follicular lymphomas, 35 mantle cell lymphomas (MCLs), and 87 mucosa-associated tissue (MALT) lymphomas (Supplementary Table 1). Three Hodgkin's-lymphoma-derived cell lines were also analysed. Interrogating more than 250,000 SNP sites, this platform permitted the identification of copy number changes at an average resolution of less than 12 kilobases (kb). The use of large numbers of SNP-specific probes is a unique feature of this platform, and combined with the CNAG/AsCNAR software, enabled accurate determination of 'allele-specific' copy numbers, and thus allowed for sensitive detection of loss of heterozygosity (LOH) even without apparent copy-number reduction, in the presence of up to 70–80% normal cell contamination[12,13].

Lymphoma genomes underwent a wide range of genetic changes, including numerical chromosomal abnormalities and segmental gains and losses of chromosomal material (Supplementary Fig. 1), as well as copy-number-neutral LOH, or uniparental disomy (Supplementary Fig. 2). Each histology type had a unique genomic signature, indicating a distinctive underlying molecular pathogenesis for different histology types (Fig. 1a and Supplementary Fig. 3). On the basis of the genomic signatures, the initial pathological diagnosis of MCL was re-evaluated and corrected to DLBCL in two cases. Although most copy number changes involved large chromosomal segments, a number of regions showed focal gains and deletions, accelerating identification of their candidate gene targets. After excluding known copy number variations, we identified 46 loci showing focal gains (19 loci) or deletions (27 loci) (Supplementary Tables 2 and 3 and Supplementary Fig. 4).

Genetic lesions on the NF-κB pathway were common in B-cell lymphomas and found in approximately 40% of the cases (Supplementary Table 1), underpinning the importance of aberrant NF-κB activation in lymphomagenesis[11,14] in a genome-wide fashion. They included focal gain/amplification at the *REL* locus (16.4%) (Fig. 1b) and *TRAF6* locus (5.9%), as well as focal deletions at the *PTEN* locus (5.5%) (Supplementary Figs 1 and 4). However, the most striking finding was the common deletion at 6q23.3 involving a 143-kb segment. It exclusively contained the *A20* gene (also called *TNFAIP3*), a negative regulator of NF-κB activation[3–7,15] (Fig. 1b), which was previously reported as a candidate target of 6q23 deletions in ocular lymphoma[16]. LOH involving the *A20* locus was found in 50 cases, of which 12 showed homozygous deletions as determined by the loss of both alleles in an allele-specific copy number analysis (Fig. 1b, Table 1 and Supplementary Table 4). On the basis of this finding, we searched for possible tumour-specific mutations of *A20* by genomic DNA sequencing of entire coding exons of the gene in the same series of lymphoma samples (Supplementary Fig. 5). Because two out of the three Hodgkin's-lymphoma-derived cell lines had biallelic *A20* deletions/mutations (Supplementary Fig. 6), 24 primary samples from Hodgkin's lymphoma were also analysed for mutations, where

[1]Cancer Genomics Project, Department of [2]Pediatrics, [3]Cell Therapy and Transplantation Medicine, and [4]Hematology and Oncology, Graduate School of Medicine, University of Tokyo, 7-3-1 Hongo, Bunkyo-ku, Tokyo 113-8655, Japan. [5]Core Research for Evolutional Science and Technology, Japan Science and Technology Agency, 4-1-8, Honcho, Kawaguchi-shi, Saitama 332-0012, Japan. [6]Department of Pediatrics, Graduate School of Medicine, Kyoto University, 54 Kawahara-cho, Shogoin, Sakyo-ku, Kyoto 606-8507, Japan. [7]Department of Pathology, Okayama University Graduate School of Medicine, Dentistry and Pharmaceutical Sciences, 2-5-1 Shikata-cho, Kita-ku, Okayama 700-8558, Japan. [8]Division of Pathology, The Cancer Institute of Japanese Foundation for Cancer Research, Japan, 3-10-6 Ariake, Koto-ku, Tokyo 135-8550, Japan. [9]Hematology Division, Hospital, and [10]Early Oncogenesis Research Project, Research Institute, National Cancer Center, 5-1-1 Tsukiji, Chuo-ku, Tokyo 104-0045, Japan. [11]Division of Immunology, Aichi Cancer Center Research Institute, 1-1 Kanokoden, Chikusa-ku, Nagoya 464-8681, Japan. [12]Gunma Children's Medical Center, 779 Shimohakoda, Hokkitsu-machi, Shibukawa 377-8577, Japan. [13]Division of Hematology, Internal Medicine, Showa University Fujigaoka Hospital, 1-30, Fujigaoka, Aoba-ku, Yokohama-shi, Kanagawa 227-8501, Japan. [14]Department of Pathology, Teikyo University School of Medicine, 2-11-1 Kaga, Itabashi-ku, Tokyo 173-8605, Japan.

©2009 Macmillan Publishers Limited. All rights reserved

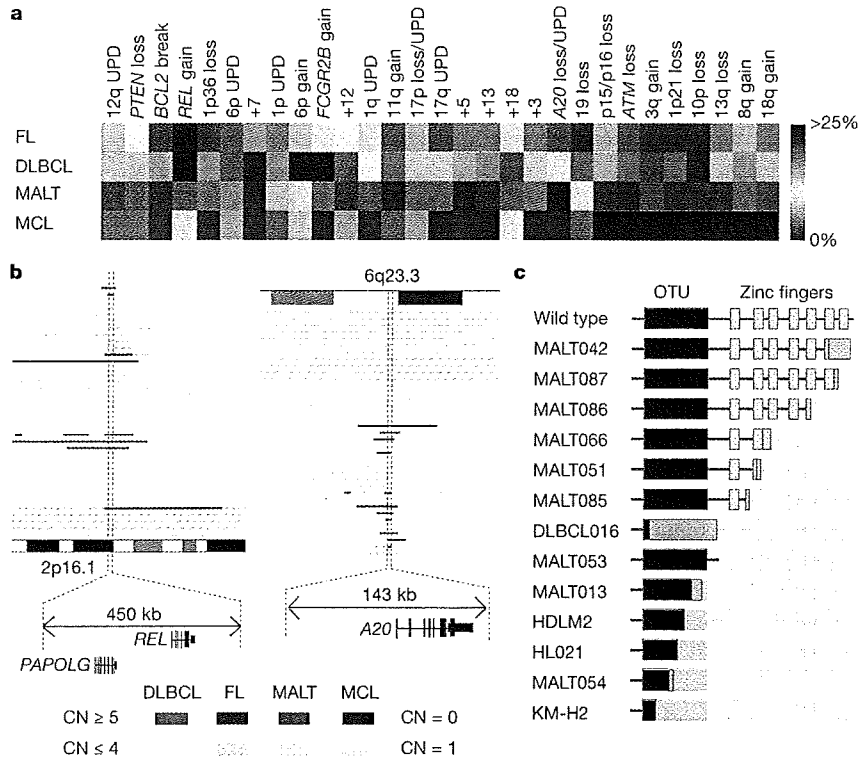

Figure 1 | Genomic signatures of different B-cell lymphomas and common genetic lesions at 2p16-15 and 6q23.3 involving NF-κB pathway genes. **a**, Twenty-nine genetic lesions were found in more than 10% in at least one histology and used for clustering four distinct histology types of B-lineage lymphomas. The frequency of each genetic lesion in each histology type is colour-coded. FL, follicular lymphoma; UPD, uniparental disomy. **b**, Recurrent genetic changes are depicted based on CNAG output of the SNP array analysis of 238 B-lineage lymphoma samples, which include gains at the *REL* locus on 2p16-15 (left panel) and the *A20* locus on 6q23.3 (right panel). Regions showing copy number gain or loss are indicated by horizontal lines. Four histology types are indicated by different colours, where high-grade amplifications and homozygous deletions are shown by darker shades to discriminate from simple gains (copy number ≤4) and losses (copy number = 1) (lighter shades). **c**, Point mutations and small nucleotide insertions and deletions in the *A20* (*TNFAIP3*) gene caused premature truncation of A20 in most cases. Altered amino acids caused by frame shifts are indicated by green bars.

genomic DNA was extracted from 150 microdissected CD30-positive tumour cells (Reed–Sternberg cells) for each sample. *A20* mutations were found in 18 out of 265 lymphoma samples (6.8%) (Table 1), among which 13 mutations, including nonsense mutations (3 cases), frame-shift insertions/deletions (9 cases), and a splicing donor site mutation (1 case) were thought to result in premature termination of translation (Fig. 1c). Four missense mutations and one intronic mutation were identified in five microdissected Hodgkin's lymphoma samples. They were not found in the surrounding normal tissues, and thus, were considered as tumour-specific somatic changes.

In total, biallelic *A20* lesions were found in 31 out of 265 lymphoma samples including 3 Hodgkin's lymphoma cell lines. Quantitative analysis of SNP array data suggested that these *A20* lesions were present in the major tumour fraction within the samples (Supplementary Fig. 7). Inactivation of *A20* was most frequent in MALT lymphoma (18 out of 87) and Hodgkin's lymphoma (7 out of 27), although it was also found in DLBCL (5 out of 64) and follicular lymphoma (1 out of 52) at lower frequencies. In MALT lymphoma, biallelic *A20* lesions were confirmed in 18 out of 24 cases (75.0%) with LOH involving the 6q23.3 segment (Supplementary Fig. 8). Considering the limitation in detecting very small homozygous deletions, *A20* was thought to be the target of 6q23 LOH in MALT lymphoma. On the other hand, the 6q23 LOHs in other histology types tended to be extended into more centromeric regions and less frequently accompanied biallelic *A20* lesions (Supplementary Fig. 8 and Supplementary Table 4), indicating that they might be more heterogeneous with regard to their gene targets. We were unable to analyse Hodgkin's lymphoma samples using SNP arrays owing to insufficient genomic DNA obtained from microdissected samples, and were likely to underestimate the frequency of *A20* inactivation in Hodgkin's lymphoma because we might fail to detect a substantial proportion of cases with homozygous deletions, which explained 50% (12 out of 24) of *A20* inactivation in other histology types. *A20* mutations in Hodgkin's lymphoma were exclusively found in nodular sclerosis classical Hodgkin's lymphoma (5 out of 15) but not in other histology types (0 out of 9), although the possible association requires further confirmation in additional cases.

A20 is a key regulator of NF-κB signalling, negatively modulating NF-κB activation through a wide variety of cell surface receptors and viral proteins, including tumour-necrosis factor (TNF) receptors, toll-like receptors, CD40, as well as Epstein–Barr-virus-associated LMP1 protein[2,5,17,18]. To investigate the role of A20 inactivation in lymphomagenesis, we re-expressed wild-type A20 under a *Tet*-inducible promoter in a lymphoma-derived cell line (KM-H2) that had no functional *A20* alleles (Supplementary Fig. 6), and examined the effect of A20 re-expression on cell proliferation, survival and downstream NF-κB signalling pathways. As shown in Fig. 2a–c and Supplementary Fig. 9, re-expression of wild-type A20 resulted in the suppression of cell proliferation and enhanced apoptosis, and in the concomitant accumulation of IκBβ and IκBε, and downregulation of NF-κB activity. In contrast, re-expression of two lymphoma-derived A20 mutants, $A20^{532Stop}$ or $A20^{750Stop}$, failed to show growth suppression, induction of apoptosis, accumulation of IκBβ and IκBε or downregulation of

©2009 Macmillan Publishers Limited. All rights reserved

Table 1 | Inactivation of A20 in B-lineage lymphomas

Histology	Tissue	Sample	Allele	Uniparental disomy	Exon	Mutation	Biallelic inactivation
DLBCL							5 out of 64 (7.8%)
	Lymph node	DLBCL008	−/−	No	–	–	
	Lymph node	DLBCL016	+/−	No	Ex2	329insA	
	Lymph node	DLBCL022	−/−	No	–	–	
	Lymph node	DLBCL028	−/−	Yes	–	–	
	Lymph node	MCL008*	−/−	Yes	–	–	
Follicular lymphoma							1 out of 52 (1.9%)
	Lymph node	FL024	−/−	No	–	–	
MCL							0 out of 35 (0%)
MALT							18 out of 87 (21.8%)
Stomach							3 out of 23 (13.0%)
	Gastric mucosa	MALT013	+/+	Yes	Ex5	705insG	
	Gastric mucosa	MALT014	+/+	Yes	Ex3	Ex3 donor site>A	
	Gastric mucosa	MALT036	+/−	No	Ex7	delintron6–Ex7†	
Eye							13 out of 43 (30.2%)
	Ocular adnexa	MALT008	−/−	No	–	–	
	Ocular adnexa	MALT017	−/−	No	–	–	
	Ocular adnexa	MALT051	+/−	No	Ex7	1943delTG	
	Ocular adnexa	MALT053	+/+	Yes	Ex6	1016G>A(stop)	
	Ocular adnexa	MALT054	+/−	No	Ex3	502delTC	
	Ocular adnexa	MALT055	−/−	No	–	–	
	Ocular adnexa	MALT066	+/−	No	Ex7	1581insA	
	Ocular adnexa	MALT067	−/−	No	–	–	
	Ocular adnexa	MALT082	−/−	Yes	–	–	
	Ocular adnexa	MALT084	−/−	Yes	–	–	
	Ocular adnexa	MALT085	+/+	Yes	Ex7	1435insG	
	Ocular adnexa	MALT086	+/+	Yes	Ex6	878C>T(stop)	
	Ocular adnexa	MALT087	+/+	Yes	Ex9	2304delGG	
Lung							2 out of 12 (16.7%)
	Lung	MALT042	−/−	No	–	–	
	Lung	MALT047	+/+	Yes	Ex9	2281insT	
Other‡							0 out of 9 (0%)
Hodgkin's lymphoma							7 out of 27 (26.0%)
NSHL	Lymph node	HL10	ND	ND	Ex7	1777G>A(V571I)	
NSHL	Lymph node	HL12	ND	ND	Ex7	1156A>G(R364G)	
NSHL	Lymph node	HL21	ND	ND	Ex4	569G>A(stop)	
NSHL	Lymph node	HL24	ND	ND	Ex3	1487C>A(T474N)	
NSHL	Lymph node	HL23	ND	ND	–	Intron 3§	
	Cell line	KM-H2	−/−	No	–		
	Cell line	HDLM2	+/−	No	Ex4	616ins29bp‖	
Total							31 out of 265 (11.7%)

DLBCL, diffuse large B-cell lymphoma; MALT, MALT lymphoma; MCL, mantle cell lymphoma; ND, not determined because SNP array analysis was not performed; NSHL, nodular sclerosis classical Hodgkin's lymphoma.
* Diagnosis was changed based on the genomic data, which was confirmed by re-examination of pathology.
† Deletion including the boundary of intron 6 and exon 7 (see also Supplementary Fig. 5b).
‡ Including 1 parotid gland, 1 salivary gland, 2 colon and 5 thyroid cases.
§ Insertion of CTC at −19 bases from the beginning of exon 3.
‖ Insertion of TGGCTTCCACAGACACACCCATGGCCCGA.

NF-κB activity (Fig. 2a–c), indicating that these were actually loss-of-function mutations. To investigate the role of A20 inactivation in lymphomagenesis *in vivo*, *A20*- and mock-transduced KM-H2 cells were transplanted in NOD/SCID/γ_c^{null} (NOG) mice[19], and their tumour formation status was examined for 5 weeks with or without induction of wild-type A20 by tetracycline administration. As shown in Fig. 2d, mock-transduced cells developed tumours at the injected sites, whereas the *Tet*-inducible *A20*-transduced cells generated tumours only in the absence of A20 induction (Supplementary Table 5), further supporting the tumour suppressor role of A20 in lymphoma development.

Given the mode of negative regulation of NF-κB signalling, we next investigated the origins of NF-κB activity that was deregulated by A20 loss in KM-H2 cells. The conditioned medium prepared from a 48-h serum-free KM-H2 culture had increased NF-κB upregulatory activity compared with fresh serum-free medium, which was inhibited by re-expression of A20 (Fig. 3a). KM-H2 cells secreted two known ligands for TNF receptor—TNF-α and lymphotoxin-α (Supplementary Fig. 10)[20]—and adding neutralizing antibodies against these cytokines into cultures significantly suppressed their cell growth and NF-κB activity without affecting the levels of their overall suppression after A20 induction (Fig. 3b, d). In addition, recombinant TNF-α and/or lymphotoxin-α added to fresh serum-free medium promoted cell growth and NF-κB activation in KM-H2 culture, which were again suppressed by re-expression of A20 (Fig. 3c, e). Although our data in Fig. 3 also show the presence of factors other than TNF-α and lymphotoxin-α in the KM-H2-conditioned medium—as well as some intrinsic pathways in the cell (Fig. 3a)—that were responsible for the A20-dependent NF-κB activation, these results indicate that both cell growth and NF-κB activity that were upregulated by A20 inactivation depend at least partly on the upstream stimuli that evoked the NF-κB-activating signals.

Aberrant activation of the NF-κB pathway is a hallmark of several subtypes of B-lineage lymphomas, including Hodgkin's lymphoma, MALT lymphoma, and a subset of DLBCL, as well as other lymphoid neoplasms[11,14], where a number of genetic alterations of NF-κB signalling pathway genes[21–25], as well as some viral proteins[26,27], have been implicated in the aberrant activation of the NF-κB pathway[14]. Thus, frequent inactivation of A20 in Hodgkin's lymphoma and MALT and other lymphomas provides a novel insight into the molecular pathogenesis of these subtypes of B-lineage lymphomas through deregulated NF-κB activation. Because A20 provides a

©2009 Macmillan Publishers Limited. All rights reserved

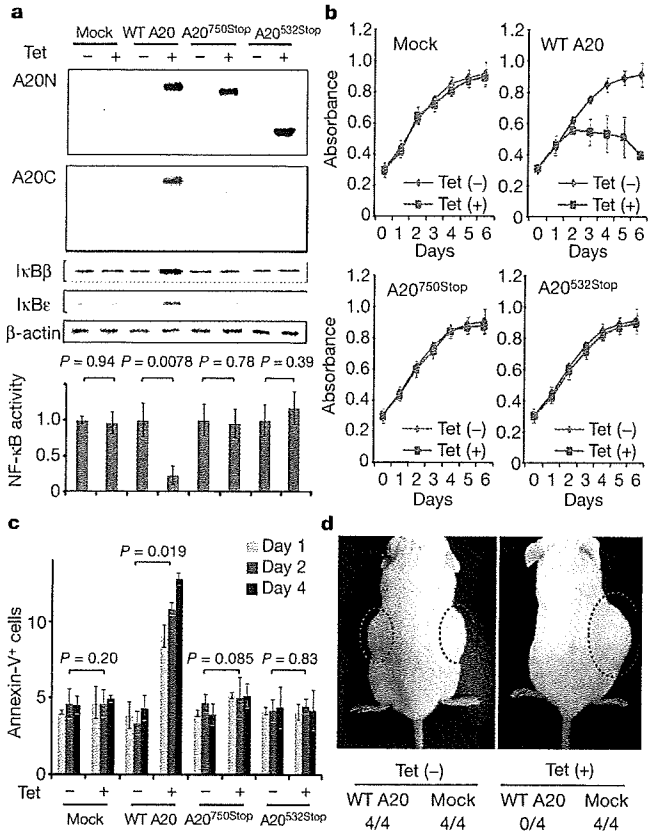

Figure 2 | Effects of wild-type and mutant A20 re-expressed in a lymphoma cell line that lacks the normal *A20* gene. **a**, Western blot analyses of wild-type (WT) and mutant ($A20^{532Stop}$ and $A20^{750Stop}$) A20, as well as IκBβ and IκBε, in KM-H2 cells, in the presence or absence of tetracycline treatment (top panels). A20N and A20C are polyclonal antisera raised against N-terminal and C-terminal A20 peptides, respectively. β-actin blots are provided as a control. NF-κB activities are expressed as mean absorbance ± s.d. ($n = 6$) in luciferase assays (bottom panel). **b**, Proliferation of KM-H2 cells stably transduced with plasmids for mock and *Tet*-inducible wild-type A20, $A20^{532Stop}$ and $A20^{750Stop}$ was measured using a cell counting kit in the presence (red lines) or absence (blue lines) of tetracycline. Mean absorbance ± s.d. ($n = 5$) is plotted. **c**, The fractions of Annexin-V-positive KM-H2 cells transduced with various *Tet*-inducible A20 constructs were measured by flow cytometry after tetracycline treatment and the mean values (±s.d., $n = 3$) are plotted. **d**, *In vivo* tumorigenicity was assayed by inoculating 7×10^6 KM-H2 cells transduced with mock or *Tet*-inducible wild-type A20 in NOG mice, with (right panel) or without (left panel) tetracycline administration.

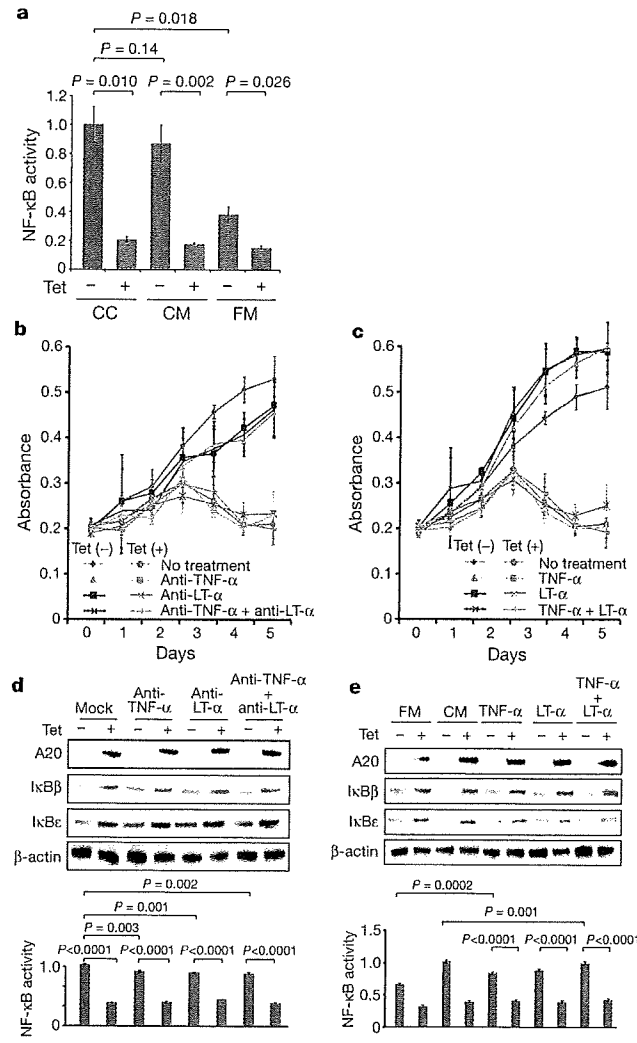

Figure 3 | Tumour suppressor role of A20 under external stimuli. **a**, NF-κB activity in KM-H2 cells was measured 30 min after cells were inoculated into fresh medium (FM) or KM-H2-conditioned medium (CM) obtained from the 48-h culture of KM-H2, and was compared with the activity after 48 h continuous culture of KM-H2 (CC). A20 was induced 12 h before inoculation in Tet (+) groups. **b**, **c**, Effects of neutralizing antibodies against TNF-α and lymphotoxin-α (LTα) (**b**) and of recombinant TNF-α and LT-α added to the culture (**c**) on cell growth were evaluated in the presence (Tet (+)) or absence (Tet (−)) of A20 induction. Cell numbers were measured using a cell counting kit and are plotted as their mean absorbance ± s.d. ($n = 6$). **d**, **e**, Effects of the neutralizing antibodies (**d**) and the recombinant cytokines added to the culture (**e**) on NF-κB activities and the levels of IκBβ and IκBε after 48 h culture with (Tet (+)) or without (Tet (−)) tetracycline treatment. NF-κB activities are expressed as mean absorbance ± s.d. ($n = 6$) in luciferase assays.

negative feedback mechanism in the regulation of NF-κB signalling pathways upon a variety of stimuli, aberrant activation of NF-κB will be a logical consequence of A20 inactivation. However, there is also the possibility that the aberrant NF-κB activity of A20-inactivated lymphoma cells is derived from upstream stimuli, which may be from the cellular environment. In this context, it is intriguing that MALT lymphoma usually arises at the site of chronic inflammation caused by infection or autoimmune disorders and may show spontaneous regression after eradication of infectious organisms[28]; furthermore, Hodgkin's lymphoma frequently shows deregulated cytokine production from Reed–Sternberg cells and/or surrounding reactive cells[29]. Detailed characterization of the NF-κB pathway regulated by A20 in both normal and neoplastic B lymphocytes will promote our understanding of the precise roles of A20 inactivation in the pathogenesis of these lymphoma types. Our finding underscores the importance of genome-wide approaches in the identification of genetic targets in human cancers.

METHODS SUMMARY

Genomic DNA from 238 patients with non-Hodgkin's lymphoma and three Hodgkin's-lymphoma-derived cell lines was analysed using GeneChip SNP genotyping microarrays (Affymetrix). This study was approved by the ethics boards of the University of Tokyo, National Cancer Institute Hospital, Okayama University, and the Cancer Institute of the Japanese Foundation of Cancer Research. After appropriate normalization of mean array intensities, signal ratios between tumours and anonymous normal references were calculated in an allele-specific manner, and allele-specific copy numbers were inferred from the observed signal ratios based on the hidden Markov model using CNAG/AsCNAR software (http://www.genome.umin.jp). *A20* mutations were examined by directly sequencing genomic DNA using a set of primers (Supplementary Table 6). Full-length cDNAs of wild-type and mutant *A20* were introduced into a

©2009 Macmillan Publishers Limited. All rights reserved

lentivirus vector, pLenti4/TO/V5-DEST (Invitrogen), with a *Tet*-inducible promoter. Viral stocks were prepared by transfecting the vector plasmids into 293FT cells (Invitrogen) using the calcium phosphate method and then infected to the KM-H2 cell line. Proliferation of KM-H2 cells was measured using a Cell Counting Kit (Dojindo). Western blot analyses and luciferase assays were performed as previously described. NF-κB activity was measured by luciferase assays in KM-H2 cells stably transduced with a reporter plasmid having an NF-κB response element, pGL4.32 (Promega). Apoptosis of KM-H2 upon A20 induction was evaluated by counting Annexin-V-positive cells by flow cytometry. For *in vivo* tumorigenicity assays, 7×10^6 KM-H2 cells were transduced with the *Tet*-inducible *A20* gene and those with a mock vector were inoculated on the contralateral sides in eight NOG mice[19] and examined for their tumour formation with ($n = 4$) or without ($n = 4$) tetracycline administration. Full copy number data of the 238 lymphoma samples will be accessible from the Gene Expression Omnibus (GEO, http://ncbi.nlm.nih.gov/geo/) with the accession number GSE12906.

Full Methods and any associated references are available in the online version of the paper at www.nature.com/nature.

Received 17 September 2008; accepted 3 March 2009.
Published online 3 May 2009.

1. Dixit, V. M. *et al.* Tumor necrosis factor-α induction of novel gene products in human endothelial cells including a macrophage-specific chemotaxin. *J. Biol. Chem.* 265, 2973–2978 (1990).
2. Song, H. Y., Rothe, M. & Goeddel, D. V. The tumor necrosis factor-inducible zinc finger protein A20 interacts with TRAF1/TRAF2 and inhibits NF-κB activation. *Proc. Natl Acad. Sci. USA* 93, 6721–6725 (1996).
3. Lee, E. G. *et al.* Failure to regulate TNF-induced NF-κB and cell death responses in A20-deficient mice. *Science* 289, 2350–2354 (2000).
4. Boone, D. L. *et al.* The ubiquitin-modifying enzyme A20 is required for termination of Toll-like receptor responses. *Nature Immunol.* 5, 1052–1060 (2004).
5. Wang, Y. Y., Li, L., Han, K. J., Zhai, Z. & Shu, H. B. A20 is a potent inhibitor of TLR3- and Sendai virus-induced activation of NF-κB and ISRE and IFN-β promoter. *FEBS Lett.* 576, 86–90 (2004).
6. Wertz, I. E. *et al.* De-ubiquitination and ubiquitin ligase domains of A20 downregulate NF-κB signalling. *Nature* 430, 694–699 (2004).
7. Heyninck, K. & Beyaert, R. A20 inhibits NF-κB activation by dual ubiquitin-editing functions. *Trends Biochem. Sci.* 30, 1–4 (2005).
8. Graham, R. R. *et al.* Genetic variants near *TNFAIP3* on 6q23 are associated with systemic lupus erythematosus. *Nature Genet.* 40, 1059–1061 (2008).
9. Musone, S. L. *et al.* Multiple polymorphisms in the *TNFAIP3* region are independently associated with systemic lupus erythematosus. *Nature Genet.* 40, 1062–1064 (2008).
10. Jaffe, E. S., Harris, N. L., Stein, H. & Vardiman, J. W. *World Health Organization Classification of Tumours. Pathology and Genetics of Tumours of Hematopoietic and Lymphoid Tissues* (IARC Press, 2001).
11. Klein, U. & Dalla-Favera, R. Germinal centres: role in B-cell physiology and malignancy. *Nature Rev. Immunol.* 8, 22–33 (2008).
12. Nannya, Y. *et al.* A robust algorithm for copy number detection using high-density oligonucleotide single nucleotide polymorphism genotyping arrays. *Cancer Res.* 65, 6071–6079 (2005).
13. Yamamoto, G. *et al.* Highly sensitive method for genomewide detection of allelic composition in nonpaired, primary tumor specimens by use of affymetrix single-nucleotide-polymorphism genotyping microarrays. *Am. J. Hum. Genet.* 81, 114–126 (2007).
14. Jost, P. J. & Ruland, J. Aberrant NF-κB signaling in lymphoma: mechanisms, consequences, and therapeutic implications. *Blood* 109, 2700–2707 (2007).
15. Durkop, H., Hirsch, B., Hahn, C., Foss, H. D. & Stein, H. Differential expression and function of A20 and TRAF1 in Hodgkin lymphoma and anaplastic large cell lymphoma and their induction by CD30 stimulation. *J. Pathol.* 200, 229–239 (2003).
16. Honma, K. *et al. TNFAIP3* is the target gene of chromosome band 6q23.3-q24.1 loss in ocular adnexal marginal zone B cell lymphoma. *Genes Chromosom. Cancer* 47, 1–7 (2008).
17. Sarma, V. *et al.* Activation of the B-cell surface receptor CD40 induces A20, a novel zinc finger protein that inhibits apoptosis. *J. Biol. Chem.* 270, 12343–12346 (1995).
18. Fries, K. L., Miller, W. E. & Raab-Traub, N. The A20 protein interacts with the Epstein-Barr virus latent membrane protein 1 (LMP1) and alters the LMP1/TRAF1/TRADD complex. *Virology* 264, 159–166 (1999).
19. Hiramatsu, H. *et al.* Complete reconstitution of human lymphocytes from cord blood $CD34^+$ cells using the NOD/SCID/γ^{null} mice model. *Blood* 102, 873–880 (2003).
20. Hsu, P. L. & Hsu, S. M. Production of tumor necrosis factor-α and lymphotoxin by cells of Hodgkin's neoplastic cell lines HDLM-1 and KM-H2. *Am. J. Pathol.* 135, 735–745 (1989).
21. Dierlamm, J. *et al.* The apoptosis inhibitor gene *API2* and a novel 18q gene, *MLT*, are recurrently rearranged in the t(11;18)(q21;q21) associated with mucosa-associated lymphoid tissue lymphomas. *Blood* 93, 3601–3609 (1999).
22. Willis, T. G. *et al.* Bcl10 is involved in t(1;14)(p22;q32) of MALT B cell lymphoma and mutated in multiple tumor types. *Cell* 96, 35–45 (1999).
23. Joos, S. *et al.* Classical Hodgkin lymphoma is characterized by recurrent copy number gains of the short arm of chromosome 2. *Blood* 99, 1381–1387 (2002).
24. Martin-Subero, J. I. *et al.* Recurrent involvement of the *REL* and *BCL11A* loci in classical Hodgkin lymphoma. *Blood* 99, 1474–1477 (2002).
25. Lenz, G. *et al.* Oncogenic *CARD11* mutations in human diffuse large B cell lymphoma. *Science* 319, 1676–1679 (2008).
26. Deacon, E. M. *et al.* Epstein-Barr virus and Hodgkin's disease: transcriptional analysis of virus latency in the malignant cells. *J. Exp. Med.* 177, 339–349 (1993).
27. Yin, M. J. *et al.* HTLV-I Tax protein binds to MEKK1 to stimulate IκB kinase activity and NF-κB activation. *Cell* 93, 875–884 (1998).
28. Isaacson, P. G. & Du, M. Q. MALT lymphoma: from morphology to molecules. *Nature Rev. Cancer* 4, 644–653 (2004).
29. Skinnider, B. F. & Mak, T. W. The role of cytokines in classical Hodgkin lymphoma. *Blood* 99, 4283–4297 (2002).

Supplementary Information is linked to the online version of the paper at www.nature.com/nature.

Acknowledgements This work was supported by the Core Research for Evolutional Science and Technology, Japan Science and Technology Agency, by the 21st century centre of excellence program 'Study on diseases caused by environment/genome interactions', and by Grant-in-Aids from the Ministry of Education, Culture, Sports, Science and Technology of Japan and from the Ministry of Health, Labor and Welfare of Japan for the 3rd-term Comprehensive 10-year Strategy for Cancer Control. We also thank Y. Ogino, E. Matsui and M. Matsumura for their technical assistance.

Author Contributions M.Ka., K.N. and M.S. performed microarray experiments and subsequent data analyses. M.Ka., Y.C., K.Ta., J.T., J.N., M.I., A.T. and Y.K. performed mutation analysis of *A20*. M.Ka., S.Mu., M.S., Y.C. and Y.Ak. conducted functional assays of mutant A20. Y.S., K.Ta., Y.As., H.M., M.Ku., S.Mo., S.C., Y.K., K.To. and Y.I. prepared tumour specimens. I.K., K.O., A.N., H.N. and T.N. conducted *in vivo* tumorigenicity experiments in NOG/SCID mice. T.I., Y.H., T.Y., Y.K. and S.O. designed overall studies, and S.O. wrote the manuscript. All authors discussed the results and commented on the manuscript.

Author Information The copy number data as well as the raw microarray data will be accessible from the GEO (http://ncbi.nlm.nih.gov/geo/) with the accession number GSE12906. Reprints and permissions information is available at www.nature.com/reprints. Correspondence and requests for materials should be addressed to S.O. (sogawa-tky@umin.ac.jp) or Y.K. (ykkobaya@ncc.go.jp).

©2009 Macmillan Publishers Limited. All rights reserved

METHODS

Specimens. Primary tumour specimens were obtained from patients who were diagnosed with DLBCL, follicular lymphoma, MCL, MALT lymphoma, or classical Hodgkin's lymphoma. In total, 238 primary lymphoma specimens listed in Supplementary Table 1 were subjected to SNP array analysis. Three Hodgkin's-lymphoma-derived cell lines (KM-H2, HDLM2, L540) were obtained from Hayashibara Biochemical Laboratories, Inc., Fujisaki Cell Center and were also analysed by SNP array analysis.

Microarray analysis. High-molecular-mass DNA was isolated from tumour specimens and subjected to SNP array analysis using GeneChip Mapping 50K and/or 250K arrays (Affymetrix). The scanned array images were processed with Gene Chip Operation software (GCOS), followed by SNP calls using GTYPE. Genome-wide copy number measurements and LOH detection were performed using CNAG/AsCNAR software[12,13].

Mutation analysis. Mutations in the *A20* gene were examined in 265 samples of B-lineage lymphoma, including 62 DLBCLs, 52 follicular lymphomas, 87 MALTs, 37 MCLs and 3 Hodgkin's-lymphoma-derived cell lines and 24 primary Hodgkin's lymphoma samples, by direct sequencing using an ABI PRISM 3130xl Genetic Analyser (Applied Biosystems). To analyse primary Hodgkin's lymphoma samples in which CD30-positive tumour cells (Reed–Sternberg cells) account for only a fraction of the specimen, 150 Reed–Sternberg cells were collected for each 10 μm slice of a formalin-fixed block immunostained for CD30 by laser-capture microdissection (ASLMD6000, Leica), followed by genomic DNA extraction using QIAamp DNA Micro kit (Qiagen). The primer sets used in this study are listed in Supplementary Table 6.

Functional analysis of wild-type and mutant A20. Full-length cDNA for wild-type *A20* was isolated from total RNA extracted from an acute myeloid leukaemia-derived cell line, CTS, and subcloned into a lentivirus vector (pLenti4/TO/V5-DEST, Invitrogen). cDNAs for mutant A20 were generated by PCR amplification using mutagenic primers (Supplementary Table 6), and introduced into the same lentivirus vector. Forty-eight hours after transfection of each plasmid into 293FT cells using the calcium phosphate method, lentivirus stocks were obtained from ultrafiltration using Amicon Ultra (Millipore), and used to infect KM-H2 cells to generate stable transfectants of mock, wild-type and mutant A20. Each KM-H2 derivative cell line was further transduced stably with a reporter plasmid (pGL4.32, Promega) containing a luciferase gene under an NF-κB-responsive element by electroporation using Nucleofector reagents (Amaxa).

Assays for cell proliferation and NF-κB activity. Proliferation of the KM-H2 derivative cell lines was assayed in triplicate using a Cell Counting Kit (Dojindo). The mean absorption of five independent assays was plotted with s.d. for each derivative line. Two independent KM-H2-derived cell lines were used for each experiment. The NF-κB activity in KM-H2 derivatives for A20 mutants was evaluated by luciferase assays using a PiccaGene Luciferase Assay Kit (TOYO B-Net Co.). Each assay was performed in triplicate and the mean absorption of five independent experiments was plotted with s.d.

Western blot analyses. Polyclonal anti-sera against N-terminal (anti-A20N) and C-terminal (anti-A20C) A20 peptides were generated by immunizing rabbits with these peptides (LSNMRKAVKIRERTPEDIC for anti-A20N and CFQFKQMYG for anti-A20C, respectively). Total cell lysates from KM-H2 cells were separated on 7.5% polyacrylamide gel and subjected to western blot analysis using antibodies to A20 (anti-A20N and anti-A20C), IκBα (sc-847), IκBβ (sc-945), IκBγ (sc-7155) and actin (sc-8432) (Santa Cruz Biotechnology).

Functional analyses of wild-type and mutant A20. Each KM-H2 derivative cell line stably transduced with various *Tet*-inducible A20 constructs was cultured in serum-free medium in the presence or absence of A20 induction using 1 $\mu g\,ml^{-1}$ of tetracycline, and cell number was counted every day. 1×10^6 cells of each KM-H2 derivative cell line were analysed for their intracellular levels of IκBβ and IκBε and for NF-κB activities by western blot analyses and luciferase assays, respectively, 12 h after the beginning of cell culture. Effects of human recombinant TNF-α and lymphotoxin-α (210-TA and 211-TB, respectively, R&D Systems) on the NF-κB pathway and cell proliferation were evaluated by adding both cytokines into 10 ml of serum-free cell culture at a concentration of 200 $pg\,ml^{-1}$. For cell proliferation assays, culture medium was half replaced every 12 h to minimize the side-effects of autocrine cytokines. Intracellular levels of IκBβ, IκBε and NF-κB were examined 12 h after the beginning of the cell culture. To evaluate the effect of neutralizing TNF-α and lymphotoxin-α, 1×10^6 of KM-H2 cells transduced with both *Tet*-inducible A20 and the NF-κB-luciferase reporter were pre-cultured in serum-free media for 36 h, and thereafter neutralizing antibodies against TNF-α (MAB210, R&D Systems) and/or lymphotoxin-α (AF-211-NA, R&D Systems) were added to the media at a concentration of 200 $pg\,ml^{-1}$. After the extended culture during 12 h with or without 1 $\mu g\,ml^{-1}$ tetracycline, the intracellular levels of IκBβ and IκBε and NF-κB activities were examined by western blot analysis and luciferase assays, respectively. To examine the effects of A20 re-expression on apoptosis, 1×10^6 KM-H2 cells were cultured for 4 days in 10 ml medium with or without *Tet* induction. After staining with phycoerythrin-conjugated anti-Annexin-V (ID556422, Becton Dickinson), Annexin-V-positive cells were counted by flow cytometry at the indicated times.

***In vivo* tumorigenicity assays.** KM-H2 cells transduced with a mock or *Tet*-inducible wild-type *A20* gene were inoculated into NOG mice and their tumorigenicity was examined for 5 weeks with or without tetracycline administration. Injections of 7×10^6 cells of each KM-H2 cell line were administered to two opposite sites in four mice. Tetracycline was administered in drinking water at a concentration of 200 $\mu g\,ml^{-1}$.

ELISA. Concentrations of TNF-α, lymphotoxin-α, IL-1, IL-2, IL-4, IL-6, IL-12, IL-18 and TGF-β in the culture medium were measured after 48 h using ELISA. For those cytokines detectable after 48-h culture (TNFα, LTα, and IL-6), their time course was examined further using the Quantikine ELISA kit (R&D Systems).

Statistical analysis. Significance of the difference in NF-κB activity between two given groups was evaluated using a paired *t*-test, in which the data from each independent luciferase assay were paired to calculate test statistics. To evaluate the effect of A20 re-expression in KM-H2 cells on apoptosis, the difference in the fractions of Annexin-V-positive cells between Tet (+) and Tet (−) groups was also tested by a paired *t*-test for assays, in which the data from the assays performed on the same day were paired.

©2009 Macmillan Publishers Limited. All rights reserved

Derivation of functional mature neutrophils from human embryonic stem cells

Yasuhisa Yokoyama,[1-3] Takahiro Suzuki,[1,2,4] Mamiko Sakata-Yanagimoto,[1-3] Keiki Kumano,[1,2] Katsumi Higashi,[5] Tsuyoshi Takato,[4] Mineo Kurokawa,[2] Seishi Ogawa,[1,4,6] and Shigeru Chiba[1,3]

[1]Department of Cell Therapy and Transplantation Medicine, University of Tokyo Hospital, Tokyo; [2]Department of Hematology and Oncology, Graduate School of Medicine, University of Tokyo, Tokyo; [3]Department of Clinical and Experimental Hematology, University of Tsukuba, Ibaraki; [4]Divison of Tissue Engineering, University of Tokyo Hospital, Tokyo; [5]Department of Clinical Hematology, School of Health Sciences, Kyorin University, Tokyo; and [6]The 21st Century COE Program, Graduate School of Medicine, University of Tokyo, Tokyo, Japan

Human embryonic stem cells (hESCs) proliferate infinitely and are pluripotent. Only a few reports, however, describe specific and efficient methods to induce hESCs to differentiate into mature blood cells. It is important to determine whether and how these cells, once generated, behave similarly with their in vivo–produced counterparts. We developed a method to induce hESCs to differentiate into mature neutrophils. Embryoid bodies were formed with bone morphogenic protein-4, stem cell factor (SCF), Flt-3 ligand (FL), interleukin-6 (IL-6)/IL-6 receptor fusion protein (FP6), and thrombopoietin (TPO). Cells derived from the embryoid bodies were cultured on a layer of irradiated OP9 cells with a combination of SCF, FL, FP6, IL-3, and TPO, which was later changed to granulocyte–colony-stimulating factor. Morphologically mature neutrophils were obtained in approximately 2 weeks with a purity and efficiency sufficient for functional analyses. The population of predominantly mature neutrophils (hESC-Neu's) showed superoxide production, phagocytosis, bactericidal activity, and chemotaxis similar to peripheral blood neutrophils from healthy subjects, although there were differences in the surface antigen expression patterns, such as decreased CD16 expression and aberrant CD64 and CD14 expression in hESC-Neu's. Thus, this is the first description of a detailed functional analysis of mature hESC-derived neutrophils. (Blood. 2009;113:6584-6592)

Introduction

Embryonic stem (ES) cells can self-renew and differentiate into cells derived from all 3 germ layers (ie, ectoderm, endoderm, and mesoderm). Both mouse and human ES cells give rise to mature blood cells of granulocyte/macrophage, erythroid, and megakaryoid lineages in vitro. For blood cell induction from ES cells, the majority of investigators use a coculturing system with mouse stromal cells such as S17[1] or OP9.[2,3] Embryoid body (EB) formation is also a commonly used method to obtain starting materials for further culture.[4-6] Cell surface antigens, such as CD45 and CD34, and colony-forming ability are used as blood cell markers. Hemangioblasts, which have the capacity to differentiate into both endothelial and blood cells, have also been produced.[7-9] Only a few studies, however, have achieved specific and effective induction of mature blood cells from ES cells, particularly human ES cells (hESCs).[10]

Human ESC-derived blood cells are potentially useful as a replacement for donation-based blood for transfusion in clinical settings, for drug discovery screening, and for monitoring drug efficacy and toxicity. The current blood donation system for transfusion is incapable of providing enough granulocytes for patients with life-threatening neutropenia, although granulocyte transfusion could have a potentially significant benefit for a certain population of severely neutropenic patients.[11,12] Given the large amount of neutrophils required for transfusion,[13] hESC-derived neutrophils might be a unique solution for this treatment demand. Therefore, the development of a highly effective method of neutrophil differentiation from hESCs is an important step for both clinical application of hESCs and granulocyte transfusion medicine.

The lack of an effective method for obtaining hESC-derived neutrophils with purity sufficient for functional analysis, however, has hampered progress in this field. Once neutrophils with a high purity can be generated from hESCs, it will be important to compare their activities with those of neutrophils produced in vivo, particularly given the fact that hESCs rarely give rise to hematopoietic stem cells in vitro,[14] and thus, that hESC-derived neutrophils might not be a progeny of hematopoietic stem cells. Here, we developed an effective method of deriving mature neutrophils from hESCs through EB formation and subsequent coculture with OP9, and analyzed their morphologic and phenotypic characteristics. We then performed functional analyses of hESC-derived neutrophils in vitro, focusing on superoxide production, phagocytosis, bactericidal activity, and chemotaxis, in comparison with peripheral blood neutrophils (PB-Neu's) obtained from healthy subjects.

Methods

Human ES cell culture and EB formation

In all experiments using hESCs, we used KhES-3[15] cells (a kind gift from Dr Nakatsuji; Kyoto University, Kyoto, Japan), which were maintained as previously described.[16] Briefly, KhES-3 colonies were cultured on irradiated mouse embryonic fibroblasts in Dulbecco modified Eagle medium/F12 (Invitrogen, Carlsbad, CA) supplemented with 20% KNOCKOUT serum

Submitted May 31, 2008; accepted March 5, 2009. Prepublished online as *Blood* First Edition paper, March 25, 2009; DOI 10.1182/blood-2008-06-160838.

An Inside *Blood* analysis of this article appears at the front of this issue.

The publication costs of this article were defrayed in part by page charge payment. Therefore, and solely to indicate this fact, this article is hereby marked "advertisement" in accordance with 18 USC section 1734.

© 2009 by The American Society of Hematology

replacer (Invitrogen) and 2.5 ng/mL human basic fibroblast growth factor (Invitrogen). The culture medium was replaced daily with fresh medium. Colonies were passaged onto new mouse embryonic fibroblasts every 6 days. To induce the formation of EBs, KhES-3 colonies were picked up using collagenase, and cultured in suspension in nonserum stem cell medium that we previously used in a hematopoietic stem cell expansion protocol.[17] After 24 hours, the colonies formed EBs, which were collected and cultured further for 17 days in Iscove modified Dulbecco medium (IMDM; Invitrogen) containing 15% fetal bovine serum (FBS), 1% nonessential amino acid (Invitrogen), 2 mM L-glutamine, 100 U/mL penicillin, 100 μg/mL streptomycin, and 0.1 mM 2-mercaptoethanol (ME) supplemented with cytokines (25 ng/mL bone morphogenic protein-4 [R&D Systems, Minneapolis, MN], 50 ng/mL stem cell factor [SCF; R&D Systems], 50 ng/mL Flt-3 ligand [R&D Systems], 50 ng/mL interleukin-6 [IL-6]/IL-6 receptor fusion protein [FP6; Kyowa Hakko Kirin, Tokyo, Japan], and 20 ng/mL thrombopoietin [TPO; Kyowa Hakko Kirin]).

Expansion of hematopoietic progenitor cells and terminal differentiation into mature neutrophils on OP9 stromal cells

OP9 cells (a kind gift from Dr Nakano; Osaka University, Osaka, Japan) were irradiated with 20 Gy and plated onto gelatin-coated 6-well tissue culture plates at a density of 1.5×10^5/well. The next day, the EBs (incubated for 18 days after the initiation of suspension culture) were trypsinized and disrupted into single cells. Cells were suspended in the progenitor expansion medium (IMDM supplemented with 10% FBS, 10% horse serum [StemCell Technologies, Vancouver, BC], 5% protein-free hybridoma medium [Invitrogen], 0.1 mM 2-ME, 100 U/mL penicillin, 100 μg/mL streptomycin, 100 ng/mL SCF, Flt-3 ligand, FP6, and 10 ng/mL TPO and IL-3 [R&D Systems]) and plated onto the irradiated OP9 cells (day 0). Each well contained up to 5×10^5 EB-derived cells. The culture medium was replaced with fresh medium on day 4.

On day 7 of the progenitor expansion phase, floating cells were collected, suspended with terminal differentiation medium (IMDM supplemented with 10% FBS, 0.1 mM 2-ME, 100 U/mL penicillin, 100 μg/mL streptomycin, and 50 ng/mL granulocyte colony-stimulating factor [G-CSF; Kyowa Hakko Kirin]), and transferred onto the newly irradiated OP9 cells. The culture medium was replaced with fresh medium on day 10. This terminal differentiation phase culture was continued for 6 or 7 days.

Preparation of normal PB-Neu's and bone marrow mononuclear cells

Human peripheral blood and bone marrow cells were obtained from healthy adult donors after obtaining informed consent in accordance with the Declaration of Helsinki. The institutional review board of the University of Tsukuba approved the use of peripheral blood neutrophils in this research. PB-Neu's were prepared as previously described.[18] The purity of the neutrophils was greater than 90%, with the remaining cells mainly eosinophils. Neutrophils were suspended in Hanks balanced salt solution (HBSS; Invitrogen) containing 0.5% bovine serum albumin (BSA) and placed at 4°C. In some experiments, peripheral blood mononuclear cells (PB-MNCs) were collected from the intermediate layer after centrifugation with Lymphoprep (Axis-shield, Oslo, Norway). Bone marrow cells were directly centrifuged with Lymphoprep, and only mononuclear cells were collected. Bone marrow mononuclear cells (BM-MNCs) were used immediately for RNA extraction.

Wright-Giemsa, myeloperoxidase, and alkaline-phosphatase staining

The morphology and granule characteristics of hESC-derived cells at the indicated days were assessed by Wright-Giemsa staining, comparing them with normal PB-Neu's. Myeloperoxidase and alkaline-phosphatase staining was performed using the New PO-K staining kit and alkaline phosphatase staining kit (MUTO PURE CHEMICALS, Tokyo, Japan). The prepared slides were inspected using an Olympus BX51 microscope equipped with a 100 × /1.30 UPlan objective lens (Olympus, Tokyo, Japan). Images were acquired with an HC-2500 digital camera and Photograb-2500 software (Fujifilm, Tokyo, Japan).

Electron microscopy

After 13 or 14 days culture, the population contained predominantly morphologically mature neutrophils, and was defined as hESC-Neu's. The hESC-Neu's and PB-Neu's were fixed in 2% paraformaldehyde/2.5% glutaraldehyde in 0.1 M phosphate buffered saline (PBS; Invitrogen) for at least 12 hours, and then postfixed in 1% osmium tetroxide in 0.1 M PBS for 2 hours. After fixation, samples were dehydrated in a graded ethanol series, cleared with propylene oxide, and embedded in Epon. Thin sections of cured samples were stained with uranyl acetate and Reynolds lead citrate. The sections were inspected using a transmission electron microscope, H7000 (Hitachi, Tokyo, Japan).

Semiquantitative RT-PCR for lactoferrin

Total RNA was obtained from hESC-derived cells of indicated culture days, PB-Neu's, PB-MNC's, and BM-MNC's using an RNeasy mini kit (QIAGEN, Hilden, Germany), and cDNA was synthesized from each RNA sample using a random primer and SuperScript III (Invitrogen) following the manufacturer's protocol. Semiquantitative polymerase chain reaction (PCR) was performed as previously described.[19] The sequence information of gene-specific primers used in reverse transcription (RT)–PCR and the PCR conditions is available upon request.

Flow cytometric analysis

Surface antigens of hESC-derived cells harvested on the indicated days were analyzed by flow cytometry using fluorescence-activated cell sorting (FACS) Aria (Becton Dickinson Immunocytometry Systems, San Jose, CA). Fc receptors on the cells were blocked with PBS containing 2% FBS and FcR Blocking Reagent (Miltenyi Biotec, Bergisch Gladbach, Germany). Antigens were stained with either fluorescein isothiocyanate (FITC)–conjugated antihuman CD13, CD64, CD11b (Beckman Coulter, Fullerton, CA), or CD14 (BD Pharmingen, San Diego, CA) antibodies; phycoerythrin-conjugated antihuman CD16, CD32, CD33 (Beckman Coulter), CD11b, or CD45 (BD Pharmingen) antibodies; or allophycocyanin-conjugated antihuman CD15, CD117 (BD Pharmingen), CD34, or CD133 (Myltenyi Biotec) antibodies. The negative range was determined by referencing the fluorescence of isotype controls. Dead cells were detected using 7-amino-actinomycin D (Via-Probe; BD Pharmingen).

Apoptosis assay

Neutrophils (hESC-Neu's and PB-Neu's) were suspended in IMDM with 0.5% BSA and incubated in 6-well plates at 37°C with 5% CO_2, with or without 50 ng/mL G-CSF. At the indicated time, neutrophils were harvested, stained with FITC-conjugated Annexin V and propidium iodide (PI) using an Annexin V-FITC Kit (Beckman Coulter), and analyzed by FACS Aria. Cells negative for both Annexin V and PI were judged as live cells.

G-CSF stimulation prior to assessing neutrophil function

Because the functions of hESC-Neu's are modified by G-CSF in the culture medium, we stimulated hESC-Neu's and PB-Neu's (PB-Neu(G+)'s) for 15 minutes at 37°C with 50 ng/mL G-CSF in the reaction medium. As a control, PB-Neu's without G-CSF stimulation (PB-Neu(G−)'s) were prepared. hESC-Neu's, PB-Neu(G+)'s, and PB-Neu(G−)'s were used for functional assays directly without changing the medium.

Detection of reactive oxygen species produced by neutrophils

Neutrophil production of reactive oxygen species was detected by flow cytometry using dihydrorhodamine123 (DHR; Sigma-Aldrich, St Louis, MO) as described previously.[20-22] Briefly, 1×10^5 hESC-Neu's, PB-Neu(G+)'s, or PB-Neu(G−)'s were suspended in 400 μL of the reaction medium (HBSS containing 0.5% BSA) per tube, and 3 tubes were prepared of each sample. Catalase (Sigma-Aldrich) at a final concentration of 1000 U/mL, 1.8 μL 29 mM DHR, and 100 μL 3.2 μM phorbol myristate

acetate (PMA; Sigma-Aldrich) were added to 1 of the 3 tubes; either no DHR or only DHR was added in the other 2 tubes as controls. Reaction medium was added to bring the final volume up to 500 μL. After 15-minute reaction at 37°C, the samples were washed twice with ice-cold reaction medium, and suspended in 200 μL reaction medium. Rhodamine fluorescence from the oxidized DHR was detected using FACS Aria.

Phagocytosis and NBT-reduction test using NBT-coated yeast cells

Phagocytosis and NBT reduction were visualized in a single set of experiments. Autoclaved Baker yeast was suspended in 0.5% NBT solution (0.5% NBT [Sigma-Aldrich] and 0.85% sodium chloride in distilled water) at a density of 1×10^8/mL. A 5-μL aliquot of this yeast suspension was added to hESC-Neu's, PB-Neu(G+)'s, and PB-Neu(G−)'s at 2.5×10^5 in 50 μL FBS. After 1 hour at 37°C, the samples were washed and stained with 1% safranin-O (MUTO PURE CHEMCALS) for 5 minutes. The samples were then washed twice and suspended in 100 μL PBS. A small aliquot of each sample was placed onto a glass slide and topped with a cover glass, and the number of ingested yeast cells and their change in color from brown to purple or black were examined using a microscope. Ingested yeast cells that changed color in the cells were counted as NBT-reaction positive, whereas those that were ingested but did not change color were counted as NBT-reaction negative. The phagocytosis rate was calculated as the percentage of neutrophils that contained one or more NBT-positive yeast cells. The phagocytosis score was calculated as the total number of positive yeast cells in 100 neutrophils. Only morphologically determined neutrophils were scored, excluding contaminating cells such as macrophages, the percentage of which was less than 15% of the total cells.

Bacterial killing assay

The bacterial killing assay was performed using *Escherichia coli* ATCC25922 as previously described[23] with some modifications. Briefly, 1×10^8 colony-forming units (CFUs) of exponentially growing bacteria were suspended in 1 mL HEPES-buffered saline with 10% human AB serum (MP Biomedicals, Irvine, CA) and opsonized at 37°C for 30 minutes. Neutrophils (hESC-Neu's, PB-Neu(G−)'s, and PB-Neu(G+)'s) were suspended in HEPES-buffered saline with 40% human AB serum at a concentration of 5×10^6/mL. The opsonized *E coli* was added to the suspension of hESC-Neu's and PB-Neu's, at a neutrophil/bacteria ratio of 2:1, or control medium. After 1-hour incubation, 50 μL of samples with and without neutrophils were diluted in 2.5 mL alkalinized water (pH 11) for lysis of neutrophils. Samples were further diluted with PBS, and duplicate aliquots were added to molten tryptic soy broth with 1.5% agar kept at 42°C, rapidly mixed, and plated on dishes. The CFUs were counted after overnight incubation.

Chemotaxis assay

Chemotactic ability was determined using a modified Boyden chamber method.[24] Briefly, 700 μL of the reaction medium (HBSS containing 0.5% BSA) with or without 10^{-7} M formyl-Met-Leu-Phe (fMLP; Sigma-Aldrich) was placed into each well of a 24-well plate, and the cell culture insert (3.0-μm pores; Falcon; Becton Dickinson, Franklin Lakes, NJ) was gently placed into each well to divide the well into upper and lower sections. Neutrophils were suspended in the reaction medium at 2.5×10^6/mL and 200 μL cell suspension was added to the upper well, allowing the neutrophils to migrate from the upper to the lower side of the membrane for 90 minutes at 37°C. After incubation, the membranes were washed, fixed with methanol, stained with Carrazi hematoxylin (MUTO PURE CHEMICALS), and mounted on the slide glass. The number of neutrophils that migrated through the membrane from the upper to the lower side was counted using a microscope with a high-power lens (× 400) in 3 fields: 2 near the edge and 1 on the center. Only mature neutrophils were counted.

Statistical analyses

Results are expressed as mean plus or minus SD. Statistical significance was determined using a 2-tailed Student *t* test. Results were considered significant when *P* values were less than .05.

Results

Effective derivation of mature neutrophils from hESCs with high purity

After initiating the suspension culture of EB-derived cells, small clusters of round-shaped cells appeared on the OP9 stromal layer around day 4. The morphology of the day-7 cells visualized with Wright-Giemsa staining suggested that they were myeloblasts and promyelocytes. On days 9 and 11, myelocytes and metamyelocytes were predominant, and on day 13 or 14, 70% to 80% of the cells appeared to be stab and segmented neutrophils (Figure 1A), with approximately 90% of the granulocytes at the metamyelocyte stage or later (Table 1). This finding indicated that hESC-derived cells differentiated into mature neutrophils by a process similar to physiologic granulopoiesis. The remaining cells appeared to be macrophages or monocytes, and cells of other lineages, such as erythroid or lymphoid cells, were not observed at any time during the culture. The number of total cells peaked around days 9 to 11, with an average 2.9-fold increase (range; 0.5- to 10.0-fold in 23 independent cultures) compared with the initial EB-derived cell number. The final yield of the cells on day 13 or 14 was 1.7-fold (range; 0.1- to 8.8-fold in 28 independent cultures). We attempted to further purify the hESC-derived mature neutrophils from the "hESC-Neu" population using density gradient methods, but higher purification could not be achieved without massively reducing the cell yield. We therefore used hESC-Neu's in the subsequent experiments.

Most (97.3% ± 1.5%) of the hESC-derived mature neutrophils defined by Wright-Giemsa staining were positive for myeloperoxidase, and the alkaline-phosphatase score of hESC-Neu's was 284 plus or minus 8.6 (Figure 1B). Under transmission electron microscopy, segmented nuclei and round cytoplasmic granules of hESC-Neu's appeared very similar to those in PB-Neu's (Figure 1C).

Some myeloid cell lines, such as HL-60, have abnormal biosynthesis of secondary granule proteins.[25,26] Thus, it is important to verify the biosynthesis of secondary granule proteins in hESC-Neu's. The levels of lactoferrin mRNA in hESC-derived cells at different stages were compared with those in PB-Neu's and BM-MNCs by semiquantitative RT-PCR (Figure 1D). Lactoferrin biosynthesis begins at the myelocyte stage and terminates by the beginning of the band stage.[25,27] Lactoferrin mRNA was not detected in PB-Neu's from some donors, but was detected in PB-Neu's from others. Human ESC–derived cells at various stages as well as BM-MNCs expressed lactoferrin mRNA. The expression level of lactoferrin mRNA in the hESC-derived cells was highest at day 10 of the induction culture and declined on days 13 and 14. These findings are consistent with the documented pattern of lactoferrin biosynthesis.

Surface antigen presentation in comparison to PB-Neu's

Surface antigen expression at each level of differentiation of hESC-derived cells was analyzed by flow cytometry (Figure 2). From days 7 to 13, the common blood cell antigen CD45 was expressed in almost all the cells. CD34, CD117, and CD133, cell surface markers on normal immature hematopoietic cells, were detected in a small population of the cells on day 7, but disappeared by day 10. Common myeloid antigens CD33 and CD15 were also highly expressed, whereas CD11b expression increased during the course of maturation. CD13 is also a common myeloid antigen, but